Universidade de Aveiro Departamento de Física
2017

Elisabet Rodríguez Cruz

Padrões de circulação na Ría de Pontevedra em situações de afloramento e afundamento

Circulation patterns of Ría de Pontevedra under upwelling and downwelling conditions

Elisabet Rodríguez Cruz

Padrões de circulação na Ría de Pontevedra em situações de afloramento e afundamento

Circulation patterns of Ría de Pontevedra under upwelling and downwelling conditions

Dissertação apresentada à Universidade de Aveiro para cumprimento dos requesitos necessários à obtenção do grau de Mestre em Ciências do Mar e da Atmosfera, realizada sob a orientação científica de Prof. Dr. Jesús Manuel Pedreira Dubert, Professor Auxiliar do Departamento de Física da Universidade de Aveiro e da Dra. Maria Rita Teixeira de Sampaio Nolasco, Investigadora da Universidade de Vigo e do CESAM.

the jury / o júri

president / presidente

Prof. Doutor José Manuel Henriques Castanheira
Professor Auxiliar da Universidade de Aveiro

examiners committee / vogais

Prof. Doutor Jesús Manuel Pedreira Dubert
Professor Auxiliar da Universidade de Aveiro (Orientador)

Prof. Doutor Joaquim Guilherme Henriques Dias
Professor Auxiliar da Universidade de Lisboa

Palavras-chave fluxo; tempo de renovação; afloramento; afundamento; EOF; Ría de Pontevedra.

Resumo

Diversos estudos tem sido realizados sobre os padrões de circulação em algumas das Rías Baixas, mas este não é o caso da Ría de Pontevedra. Ao longo desta tese tentaremos completar os conhecimentos sobre esta Ría. Uma configuração do sistema ROMS-AGRIF foi utilizada neste estudo, sendo esta validada com base na comparação com dados de temperatura e salinidade medidos semanalmente pelo INTECMAR. A analise realizada baseia-se no estudo de três episódios representativos da circulação: um de afloramento e dois de afundamento, um destes com caudal do río Lérez significativo.

Foram ainda analisadas séries temporais de fluxos e de tempos de renovação através de diversas secções. Foi analisada a correlação entre estas séries e os parâmetros forçadores (ventos e caudais dos rios). Foi realizado um estudo utilizando técnicas de funções empíricas ortogonais aplicado ao campo de velocidades normal às secções.

Os eventos de afloramento são caracterizados por um reforço da circulação positiva na Ría, consistente com os fluxos de saída pela camada superior e fluxos de entrada pela camada inferior do canal principal da Ría, e com fluxos de entrada pela boca norte e os fluxos de saída pela boca sul. Nos eventos de afundamento o comportamento é oposto ao anterior. São discutidas evidências de recirculação vertical em forma de células no sentido dos ponteiros do relógio na zona externa da Ría, associado à subdução de águas oceânicas que entram na Ría pela camada superior. Este fenómeno parece criar uma zona de bloqueio no meio do eixo da Ría, que pode ser um mecanismo responsável pelo desenvolvimento das denominadas marés vermelhas. Os fluxos para o evento de afundamento são superiores aos dos eventos de afloramento. O tempo de renovação é próximo dos 2 dias para o afundamento e dos 4 dias para o afloramento.

O estudo por funções empíricas ortogonais confirma a circulação descrita durante os episódios de afloramento e afundamento discutidos neste trabalho. A previsão das condições físicas na Ría de Pontevedra é importante para a compreensão dos processos associados ao desenvolvimento de marés vermelhas.

Keywords flux; flushing time; upwelling; downwelling; EOF; Ría de Pontevedra.

Abstract

Circulation patterns inside some of the Rías Baixas have been widely studied, but this is not the case of the Ría de Pontevedra. Through this thesis, we try to enhance the knowledge about the circulation pattern of this Ría. A ROMS-AGRIF system configuration was used in this study. This configuration was validated through the comparison with weekly temperature and salinity data measured by INTECMAR. The analysis done in this work is based on the study of three representative events of the circulation patterns: one upwelling event and two downwelling events, one of them with Lérez river flow increase. Also, was analyzed temporal series of fluxes and flushing times through the external mouths and the correlations between these series and the forcing parameters (winds and average of the rivers flow). An EOF's study was applied to the subinertial normal velocities at the sections.

Upwelling events are characterized by a reinforcement of the positive estuarine circulation, consistent with surface layer outflows and deep layer inflows at the main channel of the Ría, and inflows/outflows at the north/south mouths. Downwelling events have an opposite behaviour to the event described before. There are evidences of the vertical mixing through clockwise circulations at the outer part of the Ría, associated with the ocean waters subduction that enter into the Ría through the surface layer. As a consequence, a blocking can be generated at the middle part of the Ría, which has been associated by other authors with the "red tides". Fluxes for downwelling events are higher than for upwelling events. Flushing times are around 2 days for downwelling and around 4 days for upwelling events. The EOF's study confirms the circulation described for upwelling and downwelling events, in this work.

The forecast of the physical conditions at Ría de Pontevedra are important for the understanding of the processes behind the production of HABs.

Contents

List of Figures

List of Tables

1. Introduction

1.1 Motivation

Estuarine and coastal regions are among the most active areas of the ocean, from the point of view of biogeochemical processes. They are boundaries among terrestrial, oceanic and atmospheric ecosystems and cover approximately 7% of the Earth's surface. Nowadays, these environments are growing three times faster than elsewhere and are among the most productive on earth, creating more organic matter each year than comparably-sized areas of forest, grassland or agricultural land. Unfortunately, those areas are under increased pressures on vital natural resources, threatening the water and land integrities.

Ecosystem services are fundamental life-support processes upon which all organisms depend (Daily et al., 1997). Estuaries are often the economic centers of coastal communities and are important centers of transport, international trade commerce, fishing, coastal recreation and tourism. These ecosystems provide critical habitat for species that are valued commercially, recreationally and culturally. Regulation and protection laws of these zones are essentials to have a better quality of waters and lands. North and northwest coasts of Spain (galaico-cantábrica area) are the second biggest ocean surface of Spain, after Canary waters. This north coast of Spain occupies 300.000 km^2 inside the Exclusive Economic Zone (EEZ), but only 250.000 ha are protected extension (Oceana, 2009), being less than 1%. Galicia only presents three marine protected spaces.

In 2001, the United Nations recognize that the gross lack of knowledge about marine environmental issues has a direct effect on any futher progress towards the resolution of the environmental hazards. Hydrodynamic processes are part of this lack of knowledge and provide oceanographic information to solve this problem has become an issue of concern over the last years. Berx et al. (2011) through ICES-WGOOFE (International Council for the Exploration of the Sea-Working Group on Operational Oceanographic products for Fisheries and Environment) conducted a questionnaire by 98 scientists from different affiliations to identifie the more required oceanographic variables. The three more important variables were temperature, salinity and currents. Reasonable values of temperature and salinity are important for the living organisms and for the estuarine productivity. Currents explain water movements that transport and disperse many essential elements for life and productivity. Currents, also play an important role in the natural environment quality. Hydrodynamic study of the estuaries is fundamental for a sustainable development of resources and for a

correct environmental management. It can be achieved through the forecast of the dispersion of wastewaters, intentionally or accidentally. Future existence of estuaries depend on how we choose to treat them today.

1.2 Aims

The main objective of this Dissertation is to describe the general patterns of circulation at Ría de Pontevedra during year 2015 and, during upwelling and downwelling events. To a better understanding of these problems, we need to achieve some aims:

- Study the oceanographic conditions that characterize an upwelling and a downwelling event.
- Study the resulting circulation at Ría de Pontevedra as response to the physical forcings.
- Investigate the mechanisms of water exchange between Ría de Pontevedra and adajcent shlef through diagnosis of circulation: fluxes and flushing times.
- Learn and apply robust statistical methods to analyze the circulation at Ría de Pontevedra, through the application of Empirical Orthogonal Functions (EOFs).
- Discuss the consequences of the circulation scenario on the ecosystem of Ría de Pontevedra.

1.3 Work structure

This Master's Dissertation is divided in six chapters. Chapter 1 contains the motivation and the aims. Chapter 2 is to describe the area of study, its features characteristics and the physical meteorological and oceanography forcings. The Chapter 3 is devoted to the description of the model used for this study, Regional Ocean Modeling System (ROMS), and to the explanation of some parameters computed for a better understanding of the circulation patterns: flux, flushing time and Empirical Orthogonal Functions (EOFs). The validation of the model and results are executed in Chapter 4. Finally, the Chapter 5 and 6 presents the discussion and the conclusions, with some suggestions for future works.

2. Study Area

A description of the Galician adjacent shelf, the Rías Baixas and the Ría de Pontevedra, our aim of study, is done on this chapter. Follow by some literature review about winds, the estuarine circulation pattern, water masses and a brief overview of tides at Ría de Pontevedra.

2.1 The Galician Adjacent shelf: Rías Baixas

Galician coast has a great extension, around 1600 km, and is surrounded by Cantabrian Sea and Atlantic Ocean. It is the northernmost limit of the Eastern North Atlantic Upwelling System, which extends from 10° to about 44° N. The adjacent shelf is narrow (30-50 km wide) and at depths of 160-180 m reached the shelf break (Bender et al., 2012) with an average slope of 0.5%. Further seaward, the 1000 m isobath is located about 50-60 km far from the shelf. According to Gomez-Gesteira et al. (2006) and Alvarez et al. (2008), Galician coast can be divided in three extensions: western coast from north of Portugal to Cape Finisterre, middle coast from Cape Finisterre to Cape Ortegal and the northern coast, approximately parallel to the equator. The major representative element of the Galician coast are the rías. A good and complete definition for ría appears in PROVIGO (1996). It is defined as "Flooded old fluvial valleys relatively shallow with a typical behavior of positive partially-mixed estuaries but highly influenced by the Northwestern (NW) Iberian Upwelling System". Along all the Galician coast exists two group of rías: Rías Baixas and Rías Altas, divided by Finisterre Cape. This thesis is focused in Rías Baixas, concretely in the second southernmost: Ría de Pontevedra.

Rías Baixas extend from 42° to 43° N and are constituted by four embayments, from the south to the north: Ría de Vigo, Ría de Pontevedra, Ría de Arousa and Ría de Muros-Noia (see Figure 2.2). They are deeper than the Rías Altas, have a trimmed profile and in this location the coastal platform smoothly descends to the ocean. The hydrodynamic response of these rías is mixed and complex due to the implication of the typical estuarine circulation and the high influence of the hydrodynamics in the adjacent shelf, for that reason Rías Baixas are not considered as regular estuaries. Evans and Prego (2003) limited the estuary definition, only to the inner parts of the rías, having the main estuarine processes confined to the inner small brackish water zone. These rías behave as partially mixed estuaries, with a two-layered residual circulation pattern with surface water leaving the ría and bottom water entering it (Álvarez et al., 2003; de Castro et al., 2000). Rías Baixas are a well known place of

production of sea species of great economical interest, especially mussels and also, they have a high industry activities. From a biological point of view, the most productives rías are Arousa and Vigo (de Castro et al., 2000; Ruiz-Villarreal et al., 2002).

2.2 Ría de Pontevedra

The Ría de Pontevedra is located on the West Galician coast (NW Spain), between 42.24° N and 42.44° N of latitude and 8.65° W and 9° W of longitude (Figure 2.2) and is the second one of the Galician Rías Baixas, starting by the south of west Galician coast. It is situated between Ría de Vigo (South) and Ría de Arousa (North). Ría de Pontevedra has a surface area of 147 km^2 and a volume of 3.45 km^3 (Aguiar Fernandez, 2016), it has a V-shaped and gets broader in the NE-SW direction. This Ría may be considered as an extension of the river Lérez valley, with a longitude of 62 km and a monthly average discharge between 2 and 80 m^3/s (de Castro et al., 2000). Lérez river is under the tidal influence and is responsible by the input of continental runoff into the Ría.

Figure 2.1: Map of the Ría de Pontevedra with some important locations. From Google Earth Pro

The Ría is described as a partially-mixed estuary (Ruiz-Villarreal et al., 2002) and "young-estuary" (surrounded by steep hills that rise to over 300 m) with a two-layered residual positive estuarine circulation (Pardo et al., 2001) during most of the year. This circulation consists in an upper layer of freshwater that flows seaward and a bottom layer of water coming from outside that flows upstream. Most of the authors describe the circulation component along the main channel, but few of them (Ruiz-Villarreal et al., 2002) report the existance of the transversal component of the currents, which usually has been considered as negligible in partially-mixed estuaries. Some authors described the different activities that take place in the Ría and can affect the composition of the estuarine waters or depend on the quality of

that. At the south of Tambo island the effluents from a paper production industry that flows to the north coast are reported by González-Quijano et al. (1991), also other effluents from a electrochemical complex exist in Ría de Pontevedra. Another important economical activities are the fishing and aquaculture industries (Pardo et al., 2001). Ría de Pontevedra has three spaces for mussel production: one inside Ría de Aldán, other near Bueu (Figure 2.1) and other from A Granxa to Tambo islet.

Some topographic structures of Ría de Pontevedra, which can affect the wind patterns and currents are shown in Figure 2.1. These are the Tambo islet, the Ría de Aldán and the Ons and Onza islands. The Tambo islet is located at the inner part of the Ría, has a conical shape, 540 m x 600 m, and a maximum height of 74 m. The Ría de Aldán is responsible for the assimetric of the Ría de Pontevedra, it is oriented in the NNW direction, located in the southern coast of the Ría and with an entrance length of 3.5 km.The Ría de Aldán has some mussel and octupus industries (Ruiz-Villarreal et al., 2002). The Ons and Onza islands divided the Ría from the adjacent shelf, the Ons island have a dimension of 5.9 km x 1.3 km and a maximum height of 128 m.

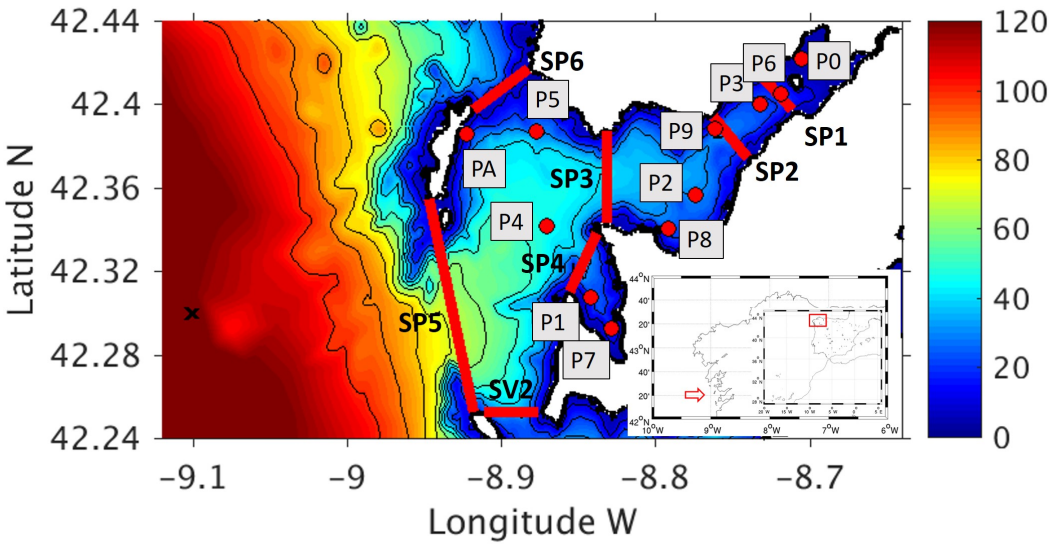

Figure 2.2: Location map of the Ría de Pontevedra with bathymetry, sections and stations. Red lines indicate sections and red dots the stations. Black cross indicates the wind measurement point. Isobaths are shown at 10 m intervals, between 10 and 110 m.

Along this thesis, Ría de Pontevedra has been considered as an estuary with three mouths (Figure 2.2). The Ons island and Cape Fagilda (Figure 2.1) delimit the north mouth (SP6) with a maximum depth of 15 m and a width of 3.65 km. The central mouth (SP5) is delimited by Ons island and Cíes islands, it has a maximum depth of 69 m and a width of 11.6 km, and the south mouth (SV2) is between Cíes island and Costa da Vela (Figure 2.1), this mouth is connected to the Ría de Vigo and has 37 m of maximum depth and 2.92 km of width. Another four more sections divided the middle and inner parts of the Ría. SP4 section is located between Ría de Aldán and Ría de Pontevedra with 35 m of maximum depth and 3.44 km of width. SP3 section is between Portonovo and Cape Udra, has 42 m of maximum depth

and 4.92 km of width. The innermost sections are SP2 and SP1, SP2 is between A Granxa and Aguete, with 30 m of maximum depth and 2.85 km of width and SP1 is located from Marín Harbour until the north coast, has 21 m of maximum depth and 2.45 km of width.

As far as is known, the circulation in Ría de Pontevedra is far from being fully understood. Some hydrographic (Álvarez et al., 2003; Dale et al., 2004; Díaz et al., 2014; Gómez-Gesteira et al., 2003; Pardo et al., 2001; Prego et al., 2001) and hydrodynamic (Aguiar Fernandez, 2016; de Castro et al., 2000, 2004; Gómez-Gesteira et al., 2001; Ruiz-Villarreal et al., 2002) studies were carried out. In most of cases it was only characterized by isolated and short events (de Castro et al., 2000, 2004; Díaz et al., 2014; Gómez-Gesteira et al., 2001; Pardo et al., 2001; Prego et al., 2001) or by using numerical model (Gómez-Gesteira et al., 2003; Dale et al., 2004; Ruiz-Villarreal et al., 2002).

2.2.1 Winds

Winds can play a major role in estuaries with enough wide in relation with its length, as mechanism driving currents. On the contrary, winds influence in long, narrow estuaries can not generate strong currents and the flow may be predominantly tidal. Shelf winds follow a seasonal pattern associated with the location of Azores anticyclone, which determines the passage of fronts in the neighborhood of the Rías Baixas. Generally, there are two typical weather regimes depending on the position of the Azores anticyclone. In winter, this meteorological structure moves to the south and the parage of low pressure system generates southwesterly winds. These direction of winds introduce masses of humid air from the ocean and when it reaches the orographic barriers produces a discharge of the humidity in the form of rain at the entrance of the Ría. On the contrary, in spring and summer the Azores anticyclone moves to the north and generates high pressures with northeasterly winds on the coast. These winds bring masses of dry air from the continent to the coast (de Castro et al., 2000; Pardo et al., 2001; Ruiz-Villarreal et al., 2002).

The wind pattern at Ría de Pontevedra was studied by de Castro et al. (2000) through a 10 years average (1986-1996) and during 1998 at Marín Harbour (Figure 2.1). These authors observed the predominance of winds in the longitudinal axis o the Ría, being a characteristic of the "young estuaries". Through the years average a predominance of NE and SW winds are observed and for one year data (1998) NE winds are predominant.

Depending on the direction of wind, the wind drag will try to pull the water in the same direction as wind, but the presence of the Coriolis force tends to balance the wind drag. In order to obtain this balance, the Coriolis force needs to be equal in magnitude to the wind drag and needs to have an opposite direction to the wind. As a result of this process and northerly direction of winds, the flow of water will be 90° to the right (left) of both the Coriolis force and the wind in the Northern Hemisphere (Southern Hemisphere). This offshore flow is the Ekman drift and decrease to zero at the coast. The water that replaces the offshore drift cannot be supplied by horizontal flow because of the coastal boundary, so it is upwelled from the deeper layers. The Figure 2.3 represents all this process and also indicates the front in

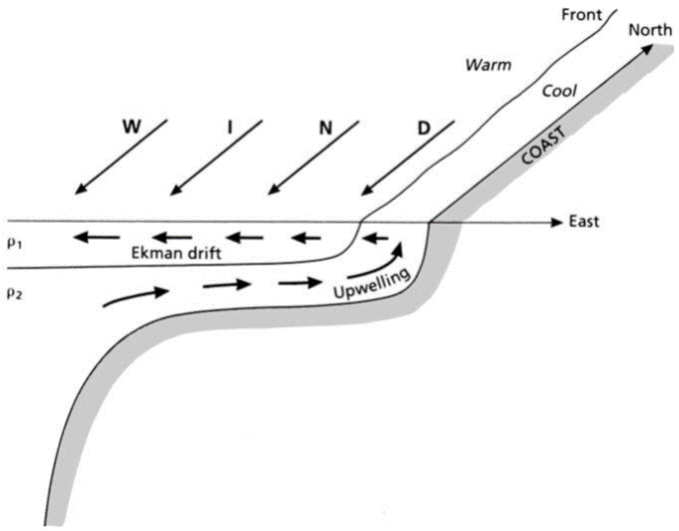

Figure 2.3: Representation of an upwelling region illustrating the Ekman drift in the upper layer being replaced near the coast by upward-moving water from the lower-layer. The winds blows from the north to the south. Source: Mann and Lazier (2006).

the near surface that separates the cooler upwelled water next to the coast from the warmer offshore water. Pardo et al. (2001) studied the variability of the driving forces into the Ría de Pontevedra and obtained that 90% of the variability can be explained by the Ekman transport at the outer part of the Ría.

2.2.2 Circulation Patterns

Ría de Pontevedra is a partially mixed estuary during most of the year with a two-layer subinertial estuarine circulation. This type of estuaries are characterized by a positive or gravitacional estuarine circulation, which is the regular situation and is enhaced in summer by coastal upwelling events, during northerly winds. The opposite situation is the negative estuarine circulation or downwelling pattern, originated by southerly winds.

de Castro et al. (2000) studied the influence of the easterly and westerly components of wind on the circulation pattern of the Ría. During summer moderate easterly winds, the water is forced to leave the estuary through surface layers and entering through the bottom layers and during strong westerlies winds, the estuarine waters are forced to enter through surface layers and can stop the normal estuarine circulation, forcing water to sink near the estuary entrance. Relative to the period of these events, Álvarez et al. (2003) carried out a one year cruise (1997-1998) at the Ría and studied a spring upwelling event that last almost 2 weeks and a winter one that last for 5 days. Rivers discharges also affects this pattern modulating its response through the buoyancy forcing. Pardo et al. (2001) applied a box-model in the Ría de Pontevedra to obtain the residual fluxes and according with their results lower rivers flow periods coincided with downwelling relaxation or upwelling events. Also, they detected the presence of two opposite circulation regimes inside the Ría divided by a front. From this front to the inner zones the Ría behaves as a typical positive estuary, and from the front to the

outer zones the entering Ekman transport originates the inversion of the circulation pattern.

2.2.3 Water Mass

Water masses have been widely studied during the past years. Prego et al. (2001) described the annual cycle of the water masses at Ría de Pontevedra through measurements from October 1997 to October 1998 with a station at the central mouth (SP5), in the outer part of the Ría. According to these authors, four different water masses in front of the Ría were identified: (1) an autumn shelf water, (2) seawater showing characteristics of the poleward current in winter, (3) subsurface shelf seawater from May to September, when the upwelling relaxes and (4) the Eastern North Atlantic Central Water (ENACW) mass, whose regular upwelling into the Ría occur in summer and it is the most described by several authors.

ENACW is considered as a subsuperficial water, between 100 and 400 m. Depending on the geographical situation, time of the year and meteorological conditions its depth can varies. Under this water mass, exists a range of 400 and 1000 m where the ENACW mixes with the Mediterranean Water (MW), due to the action of this process at the bottom and the winter cooling at the surface, the characteristics of ENACW are restricted. Galician coast has two branches of ENACW (Rios et al., 1992) from different sources: ENACW$_p$ with a subpolar origin and ENACW$_t$ with a subtropical origin. ENACW$_t$ is observed in the west Galician coast. It is formed at 35° N (Front of Azores), as a result of the subduction of gross superficial waters, generated by a high evaporation, a winter cooling and the east transport through the Azores current. It branche has temperatures of 13.13-18.50 °C and salinities of 35.80-36.75 (Rios et al., 1992).

Predominants summer northerly winds, make a displacement of superficial waters and allow the elevation of rich-nutrients ENACW (Álvarez et al., 2003; de Castro et al., 2000; Ruiz-Villarreal et al., 2002). The elevation will be more easier with a thinner superficial layer. Ría de Pontevedra tends to be more productive during this process, which brings three more times nutrients through bottom layers and then it is turn into organic matter after entering in the biological cycle.

2.2.4 Tides

Tides are one of the forcings that affect flows in Ría de Pontevedra. They can convert the tidal currents in an important source of energy and allow to treat tides as an agent of transport. Tides are produced by variations in gravitational forces caused by changes in the position and distance of the Sun and the Moon relative to points on the Earth's surface. Tides can be classified in spring and neap tides. Spring tides are large tides and are produced with full and new moon, when gravitational forces of the Sun and the Moon act together. Opposite effects (half way between full and new moon) create neap tides (minimal tides).

This forcing has been studied by some authors at Ría de Pontevedra, as Aguiar Fernandez (2016); de Castro et al. (2000) and Ruiz-Villarreal et al. (2002). They described tidal forcing at Ría de Pontevedra as mesotidal with a tidal range of 2.5 m in average and mainly semi-

diurnal with M_2, being the more significant harmonic component (1.1 m of amplitude), and modulated over the spring-neap cicle by S_2 and N_2. Ruiz-Villarreal et al. (2002) also reported amplitudes of S_2 and N_2 around 0.3 m and 0.2 m, respectively. A significant presence of the diurnal component K_1 is described by Aguiar Fernandez (2016) during the summer at the north mouth. There is no marked dominance of ebb or flood tide processes, but longer durations of flood was reported. Tidal velocities have a typical mean of 0.05-0.1 m/s, with maximum velocities around 0.3 m/s (Ruiz-Villarreal et al., 2002). Effect of tides was not take into account for this work, having subinertial variables through the application of a filter, that will be described in subsection 3.1.1.

3. Methodology

The purpose of this chapter is to make a global description of the main study tool, its configuration and the choice of some parameters of the model. In the first part, we will make a brief description of the numerical ocean model and its configuration. In the second and third parts, we will introduce a summary of the variables and of the statistical methods used in this study, which will be useful to analyze spatial and temporal variabilities of the data.

3.1 Numerical Ocean Model

The Regional Ocean Modeling Systems (ROMS) (Shchepetkin and McWilliams, 2003, 2005) is a member of a general class of three-dimenasional, split-explicit, free surface, terrain-following s-coordinate numerical model designed to resolve regional oceanic systems. This new generation of ocean circulation model solves the Reynolds-averaged Navier-Stokes equations using the hydrostatic and Boussinesq approximations, coupled with advection/diffusion equations for potential temperature and salinity, and the nonlinear UNESCO equation of state. These equations of motion in Cartesian coordinates, following the Boussinesq and hydrostatic approximations, take the form:

$$\frac{\partial u}{\partial t} = -u\frac{\partial u}{\partial x} - v\frac{\partial u}{\partial y} - w\frac{\partial u}{\partial z} + fv - \frac{\partial \phi}{\partial x} + \mathfrak{F}_{\mathfrak{u}} + \mathfrak{D}_{\mathfrak{u}} \tag{3.1}$$

$$\frac{\partial v}{\partial t} = -u\frac{\partial v}{\partial x} - v\frac{\partial v}{\partial y} - w\frac{\partial v}{\partial z} - fu - \frac{\partial \phi}{\partial y} + \mathfrak{F}_{\mathfrak{v}} + \mathfrak{D}_{\mathfrak{v}} \tag{3.2}$$

$$\frac{\partial T}{\partial t} = -u\frac{\partial T}{\partial x} - v\frac{\partial T}{\partial y} - w\frac{\partial T}{\partial z} + \mathfrak{F}_{\mathfrak{T}} + \mathfrak{D}_{\mathfrak{T}} \tag{3.3}$$

$$\frac{\partial S}{\partial t} = -u\frac{\partial S}{\partial x} - v\frac{\partial S}{\partial y} - w\frac{\partial S}{\partial z} + \mathfrak{F}_{\mathfrak{S}} + \mathfrak{D}_{\mathfrak{S}} \tag{3.4}$$

$$\rho = \rho(T, S, P) \tag{3.5}$$

$$\frac{\partial \phi}{\partial z} = -\frac{\rho g}{\rho_0} \tag{3.6}$$

$$0 = \frac{\partial u}{\partial x} + \frac{\partial v}{\partial y} + \frac{\partial w}{\partial z} \tag{3.7}$$

The momentum balance in the x and y directions are expressed by equations (3.1) and (3.2), whilst equations (3.4) and (3.3) express the time evolution of temperature and salinity, where *x, y, z* are the Cartesian coordinates; *u, v, w* are the velocity $\vec{u}$ Cartesian components; f is the Coriolis parameter; ϕ is the dynamic pressure, expressed by $\phi = (\frac{P}{\rho_o})$; $\rho = \rho_o + \rho'$ is the water density (ρ_o the average density and ρ' the perturbation); g the acceleration of gravity; $\mathfrak{F}$ and $\mathfrak{D}$ are the friction and dissipation. The non-linear equation of state is represented by equation (3.5). Equation (3.6) represents the hydrostatic approximation to the momentum balance in the vertical direction, limits to the balance between the pressure gradient and the buoyancy forces. Under the Boussinesq approximation, the density variations were taken into account for the vertical momentum equation (3.6), but neglected in the others momentum equations. The continuity equation is expressed at the equation (3.7).

The vertical boundary conditions are described as follow:

at the surface z=ζ

$$\mathrm{K}_M \frac{\partial u}{\partial z} = \tau_s^x \tag{3.8}$$

$$\mathrm{K}_M \frac{\partial v}{\partial z} = \tau_s^y \tag{3.9}$$

$$\mathrm{K}_T \frac{\partial T}{\partial z} = \frac{Q_T}{\rho_0 C_p} \tag{3.10}$$

$$\mathrm{K}_S \frac{\partial S}{\partial z} = \frac{(E-P)S}{\rho_0} \tag{3.11}$$

$$w = \frac{\partial \zeta}{\partial t} + u\frac{\partial \zeta}{\partial x} + v\frac{\partial \zeta}{\partial y} \tag{3.12}$$

at the bottom z=-h

$$\mathrm{K}_M \frac{\partial u}{\partial z} = \tau_b^x \tag{3.13}$$

$$\mathrm{K}_M \frac{\partial v}{\partial z} = \tau_b^y \tag{3.14}$$

$$\mathrm{K}_T \frac{\partial T}{\partial z} = 0 \tag{3.15}$$

$$\mathrm{K}_S \frac{\partial S}{\partial z} = 0 \tag{3.16}$$

$$w = -u\frac{\partial H}{\partial x} - v\frac{\partial H}{\partial y} \tag{3.17}$$

where ζ is the free surface elevation; K_M, K_T, K_S are the vertical turbulent mixing coefficients; τ_s^x, τ_s^y are the surface wind stress components; τ_b^x, τ_b^y are the bottom stress components, linearly parameterized and described as $\tau_b^x = rv_b$ where v_b stands for the velocity at the deepest level and r=3x10^4 m/s; Q_T is the surface heat flux; C_p is the heat capacity of the ocean; *E-P* is the evaporation minus precipitation; H is the resting thickness of the water column. Equations 3.8 and 3.9 indicate wind stress at the surface and equations 3.13 and 3.14 at the bottom. Heat fluxes are represented by equations 3.10 (surface) and 3.15 (bottom), and salinities fluxes by equations 3.11 (surface) and 3.16 (bottom). Equations 3.12 and 3.17 describe the vertical velocity at the surface and at the bottom, respectively.

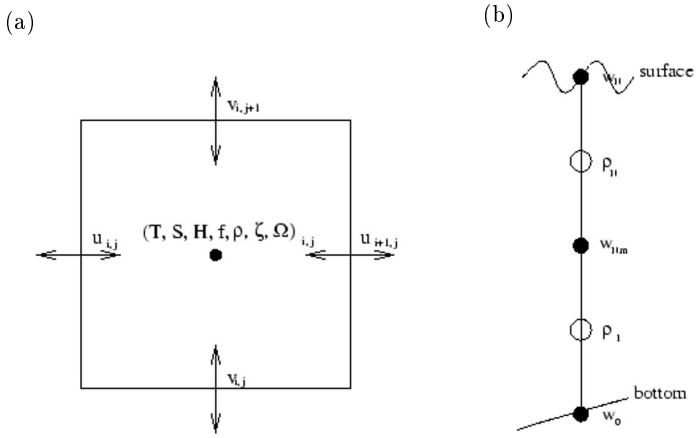

Figure 3.1: Position of the variables in a s-coordinate system (a) on the Arakawa horizontal C-grid and (b) on the staggered vertical grid. From Penven Pierrick (2000).

An optimized configuration of the ROMS with embedded nesting capabilities through Adaptive Grid Refinement In Fortran (AGRIF) package (Debreu et al., 2012) is used to simulate the exchange of properties between oceanic and estuarine waters at Ría de Pontevedra. This package is an online two-way nesting procedure which allows the use of embedded domains with increasing resolution. The domains and resolutions are described in the next subsection.

One of the advantages of the ROMS are the terrain-following or σ coordinates, its means that all the locations with different depths, from the coast to the higher depths, have the same number of levels. Consequently, a non-linear stretching factor is applied to the surface (θ_s) and to the bottom (θ_b), in order to generate a more uniform vertical resolution near the surface or the bottom, hence a better representation of the mixed layer and the thermocline is done. In the horizontal direction is adopted an Arakawa "C" grid, as we can see in Figure 3.1a, where u and v (components of the velocity vectors) are defined on the grid lines and all the other variables inside each grid cells (temperature (T), salinity (S), the resting thickness of the water column (H), the Coriolis parameter (f), the density (ρ), the free surface elevation

(ζ) and the vertical velocity (Ω)). The staggered grid applied to the horizontal dimension is also applied to the vertical (Figure 3.1b).

3.1.1 Configuration

A realistic simulation to resolve the circulation at Ría de Pontevedra was set up by R. Nolasco in the framework of Mytiga project. The Figure 3.2b shows the three domains designed for the AGRIF two way nesting algorithm: a first domain (FD), a second domain (SD) and a third domain (TD). A large domain (LD; Figure 3.2a), from 12.5° W to 5.5° W and from 34.4° N to 45.5° N, with a grid resolution of 1/27° (ca. 3 km) was created to provide initial and boundary conditions through offline nesting to the FD. The LD has been used by Nolasco et al. (2013) to describe the ocean circulation of the Western Iberian Margin (WIM) and by Nolasco et al. (in review) to the study of the marine population connectivity by the cross-validation of independent estimates. The FD, has a horizontal resolution of 1/50° (ca. 1.6 km) and extends from 11.5° W to 7° W and from 40.5° N to 45° N. The SD, designed to solve inter-Ría and shelf circulation, has a horizontal resolution of 1/150° (ca. 0.550 km) and cover a region from 9.91° W to 8.55° W and from 41.79° N to 43° N. The TD, that is used in this work, extends from 9.14° W to 8.59° W and from 42.09° N to 42.69° N, has the bigger resolution, 1/450° (ca. 180 m), and presents 30 σ vertical levels (θ_b=0 and θ_s=5). The minimum height considered for the water column is 5 meters (h_{min}=5 m). The initial boundary conditions (BC) to FD domain are taken from LD domain, whose BC are described in Nolasco et al. (2013).

There were different input forcings applied to the ROMS model. The currents used in this study results from a numerical configuration of the ROMS model (Shchepetkin and McWilliams, 2005), for the three southernmost Galician Rías: Vigo, Pontevedra and Arousa. This configuration was setup from a system of nested configurations in order to properly solve the two way exchange between the Rías and the coastal ocean. The configuration is forced by wind stress extracted from the Weather Research&Forecasting (WRF) model provided by MeteoGalicia (www.meteogalicia.es) for the year 2015. The bathymetry data were available through the RAIA consortium. A correction near the slope and a smoothing to fullfill the topographic r=δh/2h criteria was applied, with r<0.2. The inflow of freshwater from the main rivers to the ocean was included from INAG, Water Institute of Portugal for the Portugal rivers (Miño and Duero) and from Augas de Galicia provided by MeteoGalicia for the Spain rivers (Ulla, Umia, Lérez, Verdugo and Miño), when available. When there were no registers of river outflow during a long period of time, the data was provided by the SWAT Hydrologycal model contains on the website of MeteoGalicia. Tidal currents input was similar to the one used by Marta-Almeida and Dubert (2006). Elevations (amplitudes and phases) and current ellipses (semi-major axis, semi-minor axis, inclination and phase) from TPXO (Egbert and Erofeeva, 2002) global tide model was applied at the open boundaries to solve tidal currents. Tidal data was obtained from OSU TOPEX/Poseidon Global Inverse Solution, TPXO (Egbert and Erofeeva, 2002). TPXO is a global model of ocean tides, which best suits

the Laplace tidal equation and data from the TOPEX/Poseidon orbit cycles. Elevations and tidal currents were provided by the model for the main semi-diurnal and diurnal constituents (M2, S2, N2, K2 and K1, O1, P1, Q1) with a resolution of 1/12° for the North Atlantic. The model outputs are temperature (T), salinity (S) and 3D velocity fields (u, v and w) and were stored every hour. Tidal influences were removed from the output data, through "pl33tn" filtering (low pass filter), having subinertial components of all variables (tide filtered). Model results were selected for year 2015 and the validation of the these results is presented in Chapter 4. It was done using Intecmar weekly stations, shown in Figure 2.2, provided by Intecmar monitoring plan (downloaded from www.intecmar.gal).

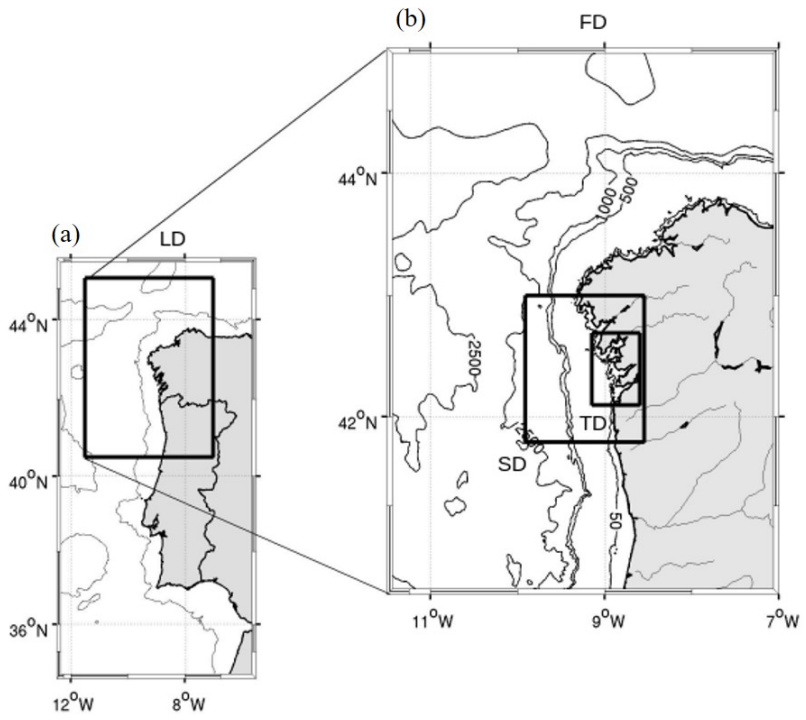

Figure 3.2: Geographic location of (a) the large (LD), (b) first (FD), second (SD) and third (TD) domains. The FD shows the 50, 500, 1000 and 2500 m bathymetric contours.

To study the behaviour of the waters from the outer part of the Ría to the innermost part, an along section was created under the construction of differents stations following the principal axis of the Ría (Figure 3.3). Some of the stations are the same as P4 (42.34° N and -8.87° W), P3 (42.40° N and -8.73° W) and P6 (42.41° N and -8.72° W). The study of this along-Ría section was done through S, T and velocities fields computed by the along section velocities (u) and vertical velocities (w) data, provided by the model. This along section constitutes the principal and longitudinal axis of the Ría de Pontevedra.

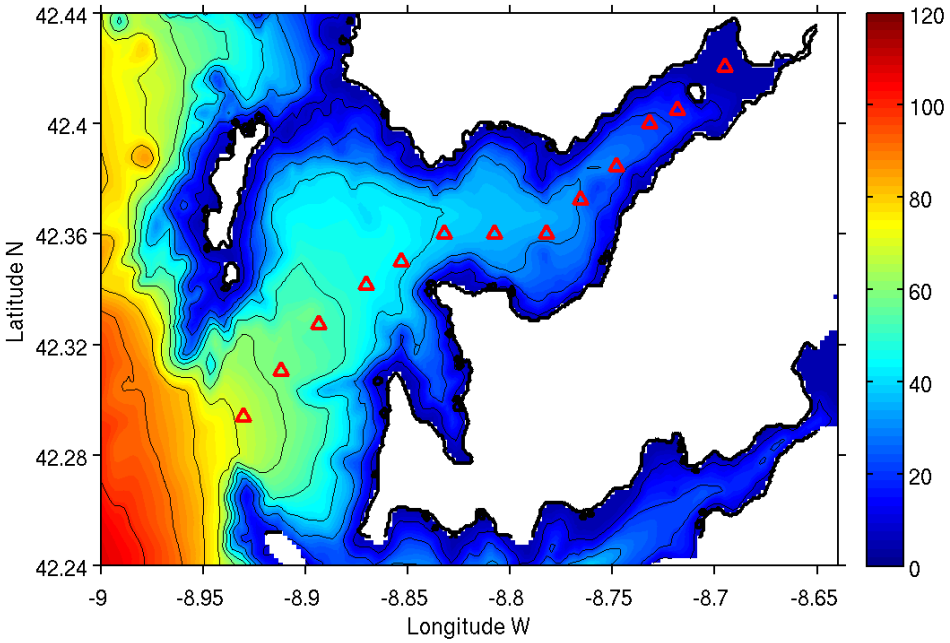

Figure 3.3: Along-ría section at Ría de Pontevedra. Isobaths are shown at 10 m intervals between 10 and 100 m.

3.2 Flux and Flushing Time: definition and computation

In order to attain a better understanding of the circulation pattern at Ría de Pontevedra two variables were computed and analyzed. Flux and flushing time are important to quantify the amount of water entering and leaving the Ría and the time that it takes to flush or drain it.

Flux (m^3/s) through a section is defined as the volume of water crossing a section per unit of time. It is expressed as:

$$Flux = \int V dA \tag{3.18}$$

where V is the normal velocity (m/s) to each section and dA is the differential element of area (m^2) of the study system. Flux was computed through external mouths (Figure 2.2), north (SP6), central (SP5) and south (SV2). We calculated three different fluxes, the inflow flux (In) as the quantity of water that is entering in the Ría, represented with positive values, the outflow flux (Out) as the quantity of water that is leaving the Ría, represented with negative values, and the net (Total) flux, which is computed as the sum of the inflow flux (positive) and the outflow flux (negative). It is the net inflow of water at the Ría in a certain time, through the three external sections.

Flushing time (Days) or turnover time is a bulk parameter. It describes general exchange characteristics of a water body and for advection-dominated flows it is defined as the ratio

between the volume of the water body, V_F, and the throughflow, which is given by the *Flux* calculated before:

$$t_F = \frac{V_F}{Flux} \tag{3.19}$$

Two flushing times were computed through external mouths (SP6, SP5 and SV2; Figure 2.2). Inflow flushing time (In), which is defined as the time needed to flush all the Ría (positive values) and outflow flushing time (Out), defined as the time needed to drain all the Ría (negative values). All variables calculated at this section are detided.

3.3 Empirical Orthogonal Functions (EOFs)

For oceanographic studies the covariability of simultaneously measured time series at different times and locations is often of interest. The spatio-temporal variability of the resulted modeled data was analyzed by Empirical Orthogonal Functions (EOFs).

The Principal Component Analysis (PCA) or commonly known as Empirical Orthogonal Functions (EOFs), can be described as the reduction in the quantity of space/temporal variables of our data set through orthogonal functions or modes. The outputs of this statistical method are spatial fields and their associated eigenvalues (relative amount of variance) and eigenvectors (temporal weightings for each time step). The chosen method to obtain the EOF eigenvectors and eigenvalues was the singular value decomposition (SVD) (Preisendorfer and Mobley, 1988). At any time in a particular point, the contribution of one EOFs is computed by multiplying the value at that location times the value of the temporal coefficient at a given instant. Then, a variable is considered to be a function *f(x,z,t)* of space and time, computed for constant space and time intervals. The data is represented as a sum of products of functions by the EOFs method:

$$f(x,z,t) = \sum F_i(x,z)G_i(t) \tag{3.20}$$

where the data distribution in space is expressed by F_i (eigenvector) and in time by G_i (time EOFs series). It gives the contribution of the respective space distribution to f at any given time. The advantage of EOFs analysis is that provides a compact description of the spatial and temporal variability of data series in terms of orthogonal functions. However, these empirical modes do not necessarily correspond to true dynamical modes or modes of physical behaviour. For example, a single physical process can be spread over more than one EOF and more than one physical process may be contributing to the variance contained in one EOF.

This method can be applied to vectors. In our study case, EOFs is applied to normal detided velocity for each section (SP6, SP5, SV2, SP3, SP2 and SP1; Figure 2.2). The vertical spatial resolution is 1 m for all the sections and the horizontal resolution varies depending on the section size, in a general way it is between 300 and 400 m, with exception of SP3 with 182 m of horizontal resolution. Out of 60 possible EOFs modes calculated, only two of them are

studied, due to a higher contribution of the variance of the studied variable. A deeper analysis of EOFs modes is achieved by a temporal evolution comparison with vertical and horizontal components of wind and rivers flow (Lérez, Verdugo and Miño). Also, a linear correlation R^2 for a moving window of 30 days is computed between two first modes and the variables used for the comparison. An Upwelling Index (UI) was computed to correlate it with different EOF modes. It is the component of the Ekman transport perpendicular to the coast expressed per unit length of coastline, and was calculated according to:

$$I_W = \frac{\rho_a C_d V_n \left|\vec{V}\right|}{f \rho_w} (m^3/km \cdot s) \tag{3.21}$$

where ρ_a is the density of air (1.22 kg/m^3); C_d is the empirical draf coefficient (1.3x10^{-3}, dimensionless); V_n is the component of wind speed parallel to the coast of magnitude $\left|\vec{V}\right|$; f is the Coriolis parameter; ρ_w is the density of seawater (1025 kg/m^3). Positive values of UI represent upwelling events and negative values represent downwelling events.

4. Results

4.1 Introduction

This chapter starts with an overview of the forcings that drive the circulation of Ría de Pontevedra: the winds and rivers inflow. Model validation is also assessed through the comparison of model results with measured available data as described below. In order to study the general circulation patterns, we selected one upwelling event and two downwelling events, one of them characterized by a river inflow increase. These events were selected based on events duration, significant wind directions and typical patterns of inflow and outflow along all the Ría. These events were studied by a along-Ría section shown in Figure 3.3 with salinity, temperature and subinertial velocities field data, constructed under the along section velocities (u) and vertical velocities (w) for all depths. Wind directions and intensities for each period are displayed to enhance the analysis. In approaching the subject, the flux and flushing time are computed. Also, a basic overview of the dominant orthogonal spatial and temporal signals is displayed by the two first modes of Empirical Orthogonal Function (EOF) and its linear correlation with different parameters.

4.2 Forcings

Estuarine circulation is driven by several forcings. In this section, forcings will be shown for a better understanding of the circulation pattern inside the Ría de Pontevedra. The studied forcings will be winds and rivers inflow evolution for the year 2015.

4.2.1 Winds

Depending on the geometry of an estuary and other factors, winds can be a prevalent forcing of the estuarine circulation. In a long, narrow estuary the flow may be predominantly tidal, and the wind effect in the currents can be reduced. On the contrary, if the estuary is enough wide in relation with its length, wind stresses can have a considerable important role in currents.

Winds for 2015 are shown in Figure 4.1 measured at 42.3° N of latitude and -9.1° W of longitude, in the outside part of the Ría (Figure 2.2). In a general way, southerly winds are prevailing during winter, and northerly winds prevail in the summer, although many variability of the wind is observed. Persistent southerly winds generate downwelling events when it last

for enough days, and northerly winds can produce upwelling of shelf waters. During year 2015 there are some long periods with nearly constant wind directions, for instance from middle of May to beginning of June (Figure 4.1a). This is a long upwelling favourable winds that lasted almost a month (27 days) and have some intervals of southerly winds in first days of June, which change the circulation during these days and recover after that. An example of a long downwelling favourable winds is shown in December (Figure 4.1b). All the month is under southerly winds with some northerly winds alternancy and decrease in wind speed. Since 13 December the southerly winds starts blowing until last days of December, lasting 17 days and being the period in which the southeast components of wind are most common. These two events are the longest of the year.

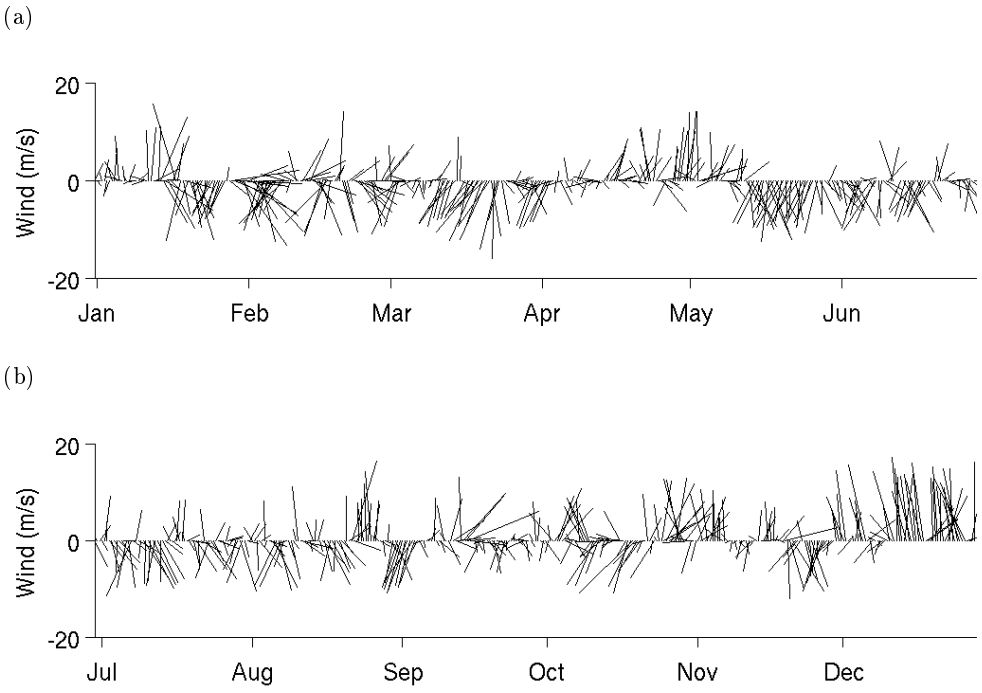

Figure 4.1: Wind directions and intensities (m/s) each four hours. Positives values indicates southerly winds and negative values indicates northerly winds. (a) From January to June and (b) from July to December.

4.2.2 Rivers

River waters have an important influence in estuaries, especially at the inner zones. The volume of freshwater in the Ría is determined by the river discharge. Miño, Lérez and Verdugo rivers flow are displayed for 2015. Rivers flow data have half a day sampling and were taken from Augas de Galicia provided by MeteoGalicia for Lérez river and from SWAT Hydrologycal (MeteoGalicia) for Verdugo and Miño rivers.

Figure 4.2 shows river flows for year 2015. The rivers represented are Miño, located between Portugal and Spain, Lérez, which discharge its waters into Ría de Vigo, and Lérez, which discharge its waters into Ría de Pontevedra. Autumn and winter are seasons with a

high number of important peaks of the main rivers, which usually take place simultaneously to downwelling favourable winds periods (Figure 4.1). These coincident events, between Lérez river flow increase and downwelling events, happen by end of January (January 29), with 82 m^3/s flow, on March 1, being that the higher flow increase (113 m^3/s), and since mid to the end of December (57 m^3/s), for winter season. In autumn, southerly winds and river flow increase occur on October 4 and 28, with 58.41 m^3/s and 69 m^3/s, respectively. Spring and summer months are characterized by upwelling favourable winds predominance, despite of that there is two periods that have downwelling events and river flow increase. One is in spring, on May 4, with 84 m^3/s, which will be studied in Section 4.5 and another in summer, on September 15, with 55 m^3/s.

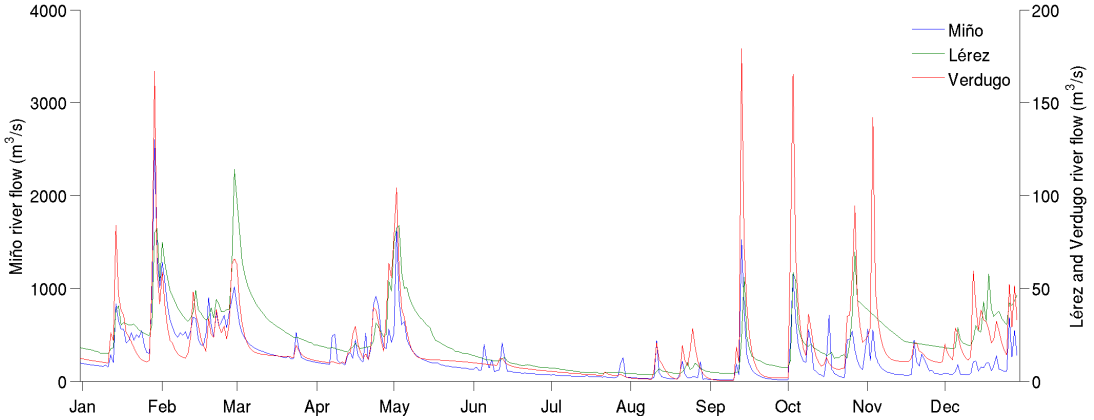

Figure 4.2: Time evolution of the river flow (m^3/s) for Lérez (green), Verdugo (red) and Miño (blue) rivers.

4.3 Model Validation

In the present study, a validation of the oceanographic model was obtained by comparison of temperature and salinity at 2 meters depth (Figure 4.3a,b) and along the water column (Figure 4.3c,d). This model evaluation was done by comparison of data predicted by the model during 2015 and weekly data measured from "Instituto Tecnoloxico para o Control do Medio Mariño de Galicia (Intecmar)", described at subsection 3.1.1.

A good agreement of the modelled data with the measured one is observed along all the year and throughout the water column (Figure 4.3). Annual cycle and daily variabilities of temperature and salinity are depicted by the model. Also, upwelling and downwelling events are captured by temperature and salinity data at P5 (near SP6; Figure 2.2) and P9 stations (near A Granxa; Figure 2.1), for example the downwelling event of beginning of May with low values of salinity and an increase in temperature (Figure 4.3a,b) and the upwelling event at middle of July, with a decrease in temperature values. This good representation can be also verified along all the water column (Figure 4.3c,d). Deep inflow of colder waters is captured during summer months (upwelling favourable winds). The homogenization of the water column is also visible in the modelled data, for example from January to April and

in June for temperature data, and from August to September for salinity data. In May, an abrupt decrease of salinity and temperature are reproduced by the model throughout the water column and in July the increase of stratification in the surface layers is also depicted.

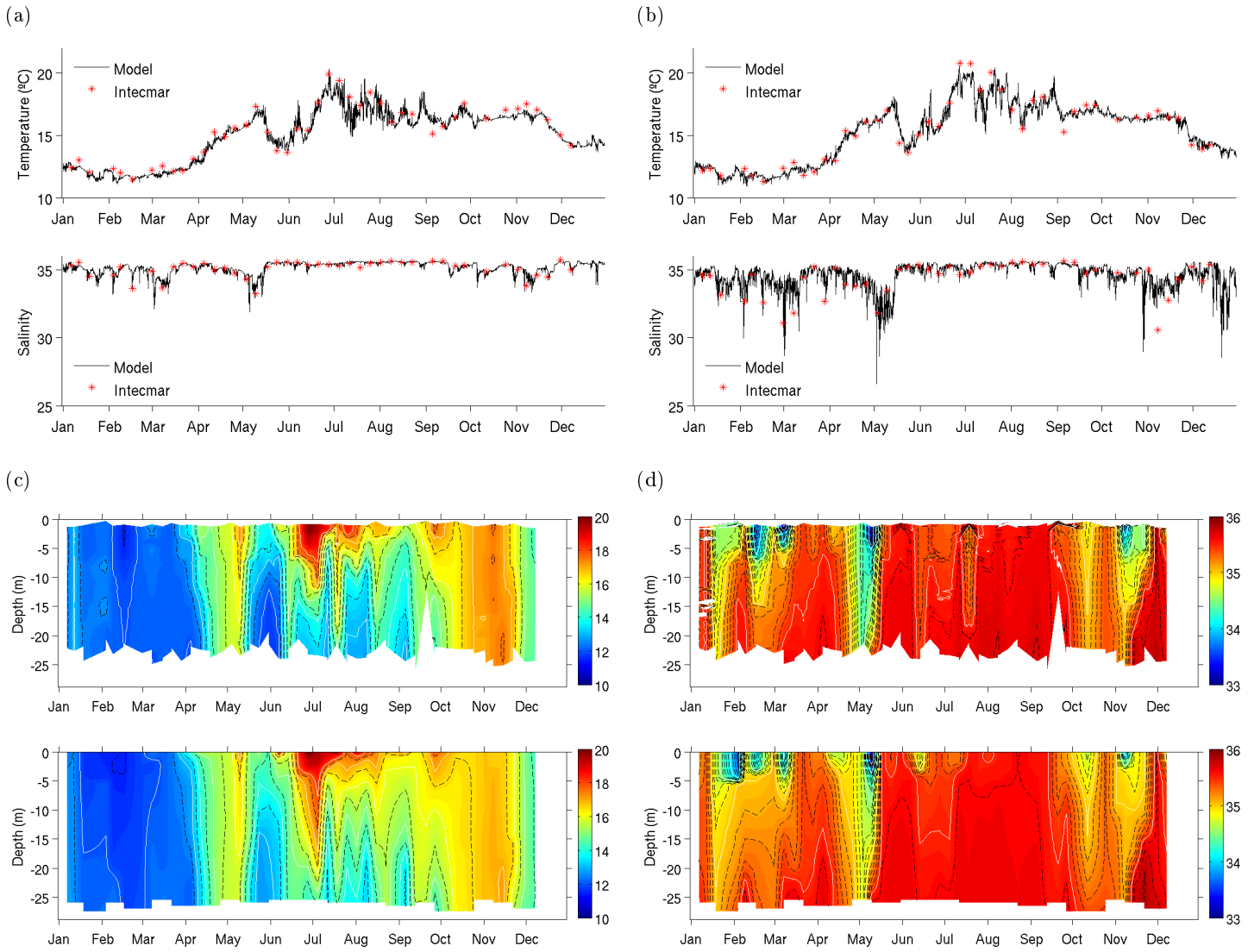

Figure 4.3: Comparison of modelled (solid line) and measured (Intecmar; red star) temperature and salinity at (a) station P5 and (b) P9. (c,d) Measured (Intecmar) temperature and salinity (top row) and (c,d) modelled temperature and salinity (bottom row) at station P5.

Additional model accuracy is also evaluated using some statistical parameters. The root mean square (RMSE) error, represents the sample standard deviation of the differences between modelled and measured values. The BIAS (Pielke, 2013) provides information about the model tendency to overestimate or underestimate the observed data, so it quantifies the systematic error of the model. The skill parameter (Willmott, 1981) is a measure of the quantitative agreement between the model and observations. It takes into account the modelled and observed deviations around the observed mean $\overline{X_{obs}}$ to estimate the model representation, and varies between 0 (no agreement) and 1 (perfect agreement). These parameters are described as follow:

$$RMSE = \sqrt{\sum_{i=1}^{N} \frac{(X_{mod} - X_{obs})^2}{N}} \tag{4.1}$$

$$BIAS = \sum_{i=1}^{N} \frac{(X_{mod} - X_{obs})}{N} \tag{4.2}$$

$$Skill = 1 - \frac{\sum |X_{mod} - X_{obs}|^2}{\sum \left(\left| X_{mod} - \overline{X_{obs}} \right| + \left| X_{obs} - \overline{X_{obs}} \right| \right)^2} \tag{4.3}$$

where X_{mod} and X_{obs} are the modelled and the measured data, respectively, and N is the number of analized data.

Table 4.1 presents the statistical parameters that quantify the model ability to reproduce the observed data for the salinity and temperature (°C), for the stations P0 to PA of Intecmar for year 2015, referred above. The RMSE parameter indicates some differences in salinities data at P0 station, the innermost station (Figure 2.2). Low BIASES are observed, with an overestimation of majority of the measured data and some of them are underestimate, as P0 and P5 stations for salinity data and P7 for temperature data. Higher differences are shown in salinity data at P0 (-0.19) and in temperature data at P6 (0.36 °C). It evidences a low systematic error of the model. Analyzing results for skill parameter, the highest disagreement is presented for salinity data at PA station (0.77), located behind Ons island and inside the ría. This low skill value can be related with the location of the station. Despite of the differences between model and measured data at some stations that are sheltered by the ría topography (Figure 2.2), we can notice that other stations close to these have good values of the statistical parameters calculated. On the basis of observations and numerical model results, we can conclude that the model has a good reproducibility of the measured data for temperature and salinity at Ría de Pontevedra.

Table 4.1: Model-data comparison calculations for salinity (S) and temperature (T; °C).

Station	Variable	RMSE	Bias	Skill (no unit)
P0	S	1.09	-0.19	0.93
	T (°C)	0.79	0.25	0.97
P1	S	0.24	0.06	0.89
	T (°C)	0.73	0.12	0.96
P2	S	0.22	0.01	0.92
	T (°C)	0.76	0.30	0.96
P3	S	0.35	0.04	0.94
	T (°C)	0.80	0.30	0.96
P4	S	0.18	0.01	0.91
	T (°C)	0.76	0.31	0.95
P5	S	0.20	-0.01	0.93
	T (°C)	0.72	0.23	0.96
P6	S	0.35	0.05	0.95
	T (°C)	0.89	0.36	0.95
P7	S	0.28	0.11	0.87
	T (°C)	0.81	-0.05	0.96
P8	S	0.24	0.04	0.91
	T (°C)	0.75	0.30	0.96
P9	S	0.32	0.04	0.93
	T (°C)	0.81	0.35	0.96
PA	S	0.35	0.09	0.77
	T (°C)	0.66	0.10	0.96

4.4 Upwelling Event

A summer upwelling event takes place from July 11 to 15. During these days, northwesterly and northeasterly wind directions blew (Figure 4.4), maximum velocities are reached on July 12, around 9.2 m/s and rest of the days the velocities are around 8 m/s. Prior to the study event, a burst of northerly winds started on July 5 and persisted until July 9, then southerly winds appeared on July 10 until the beginning of the upwelling event.

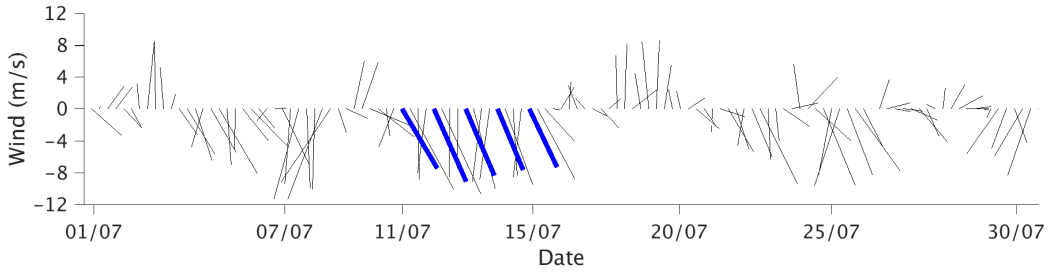

Figure 4.4: Intensities and directions of wind (m/s) during July with the summer upwelling event (blue) represented. Positives values indicate a northward component and negative values indicate a southward component.

Figure 4.5 describes the general circulation pattern during this upwelling event at the Ría through different sections. In a general way, shallower external mouths respond with a single direction of circulation, an inflow at the north mouth (SP6) and an outflow at the south mouth (SV2). Two-layered circulation with a surface outflow and a deep inflow is observed at the main channel sections of the Ría (SP5, SP3, SP2 and SP1), the level of no-motion between these layers are around 15 m depth for central mouth (SP5); for SP3 section is about 25 m depth at the north side and 10 m depth at the south side of the section; for SP2 and SP1 is around 5 m depth.

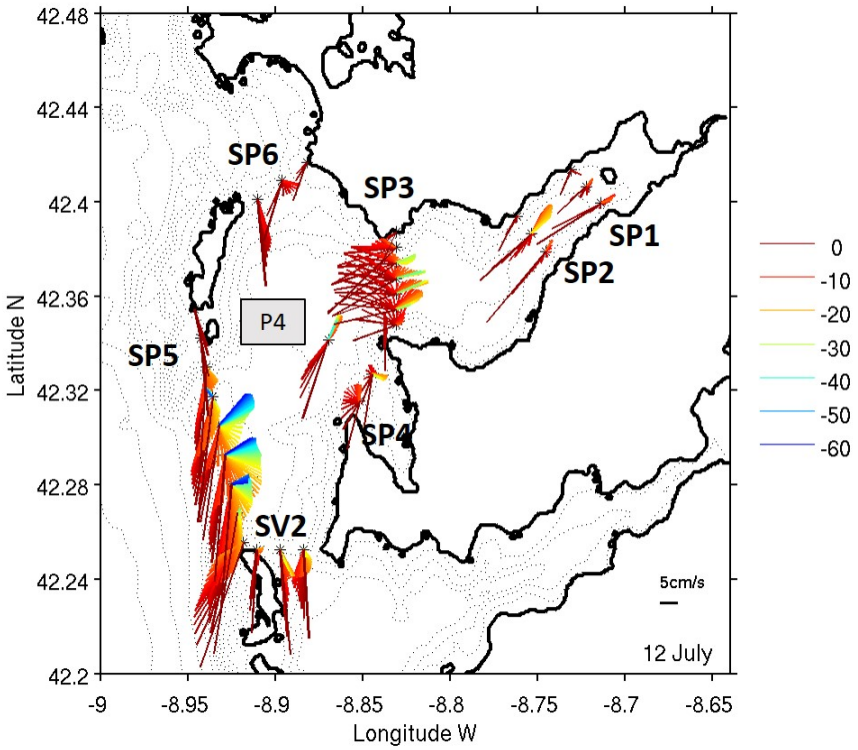

Figure 4.5: Subinertial velocities (cm/s) across sections and station P4 for July 12 at 13 hours. The depth of the arrows correspond to the scale of colors of the colorbar.

The typical estuarine pattern described above (Figure 4.5) with outflow/inflow through the surface/deep layers, will now be analyze through the along-Ría section (see Figure 3.3) in which the upwelling event will be studied based on the time evolution of T, S and subinertial velocities obtained by u (along section velocity) and w (vertical velocity). At first day of the event (July 11), Figure 4.6a,b, the T, S fields corresponds to a state of nearly no motion, because the isotherms and isohalines are nearly flat. Signal of river inflow can be observed to be confined to the inner portion of the Ría with low values of salinity ($<$35.2). Also, evidences of surface offshore flow, consequence of the Ekman dynamics can be inferred, although few evidences of deep inshore flow at the outer Ría can be observed by the rising of the 35.65 and 14 °C isolines and this motion continues in the direction of the head of the Ría. The next day (July 12), Figure 4.6c,d, the set up of the Ekman flow at the surface is visible through the offshore transport of the river plume, while below the inshore flow is well established,

associated to an upwelling of the T and S fields of about 10 m depth in one day, with an estimated velocity of 0.11 mm/s, which is comparable to the observed velocities. This upwelling squeezed the surface layers, increasing the stratification below the surface. By day July 13, the surface stratification continues to increase being particularly noticed at -8.85° W, while colder waters, around 13 °C, appear near the mouth of the Ría. This situation keeps by the next day, July 14. By the end of the event, July 15 (Figure 4.6i,j), the inner Ría is highly surface stratified in T and S, and below was replaced by colder waters, with 13-14 °C.

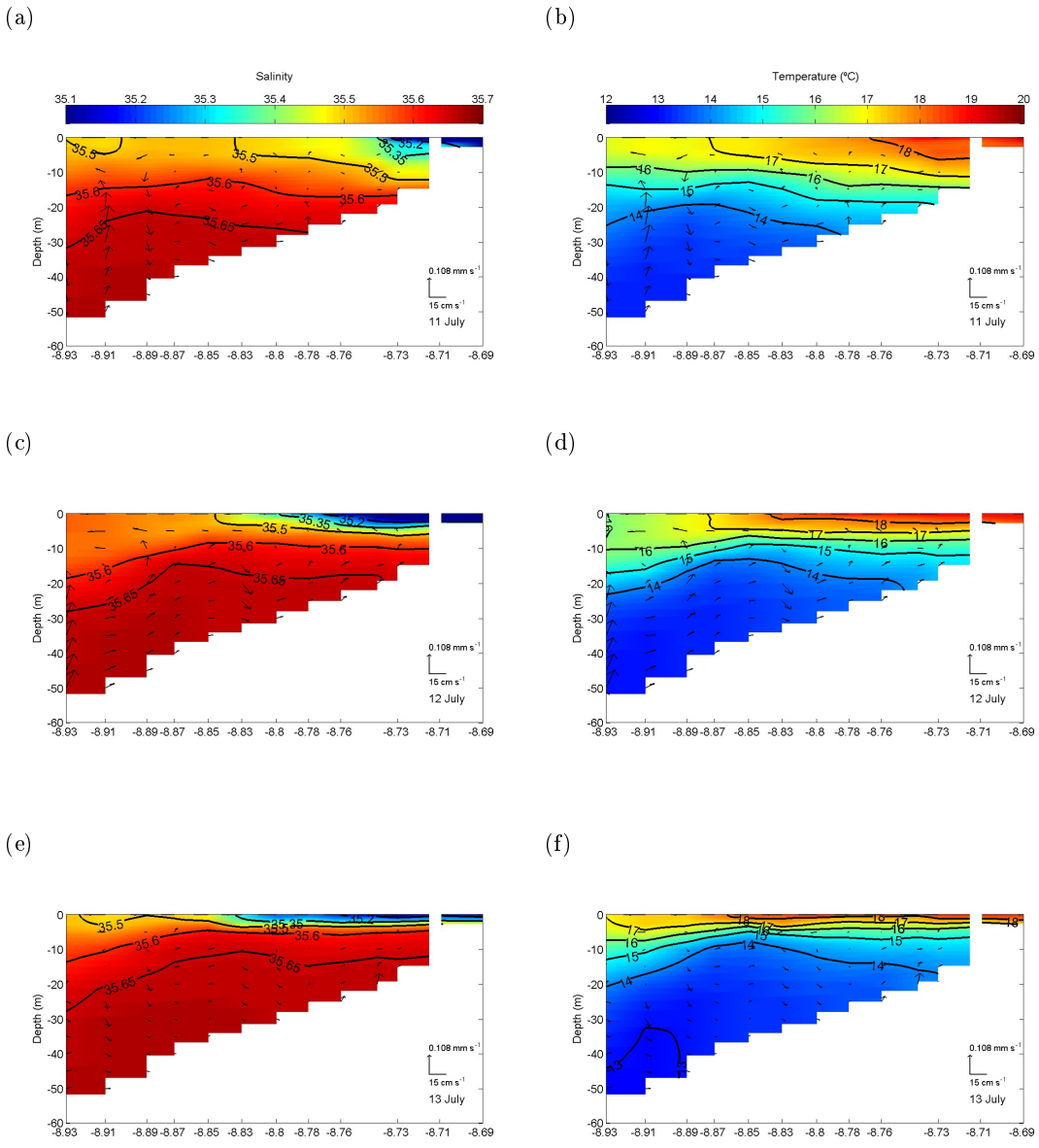

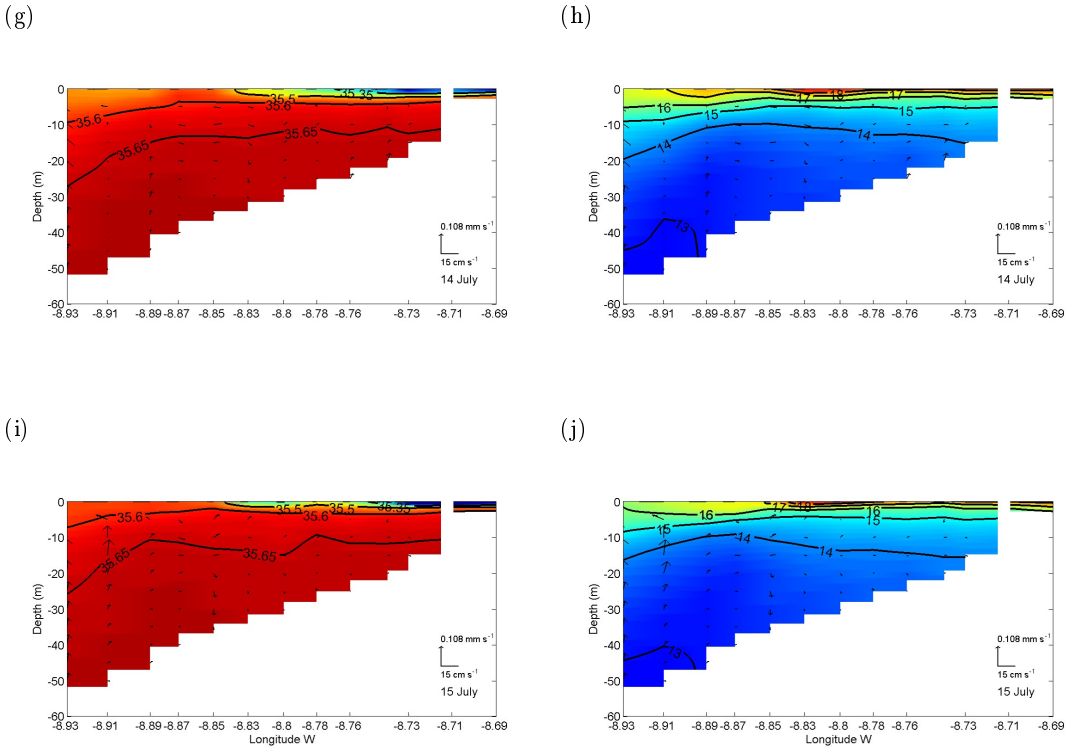

Figure 4.6: Along-Ría section for salinity (a, c, e, g, i) and temperature (°C; b, d, f, h, j) data with along and vertical subtidal velocities (cm/s and mm/s; black arrows) on July 11, 12, 13, 14, 15. The sampling transect is shown in Figure 3.3.

4.5 Downwelling Event

The summer months were also chosen to study a downwelling event, which happens from August 23 to 28. Notice that no Lérez river flow is observed during this period. Summer downwelling event is characterized by southerly winds (Figure 4.7). Higher velocities are reached on August 23, 26 and 27, with 16, 12 and 14 m/s, respectively. August 25 and

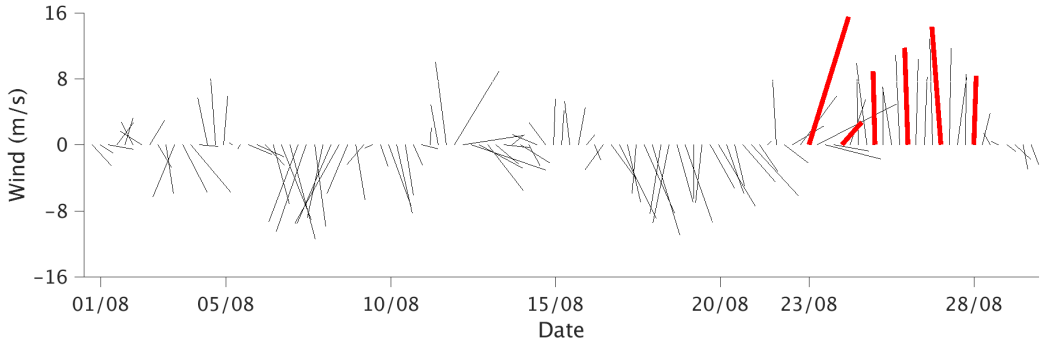

Figure 4.7: Intensities and directions of wind (m/s) during the downwelling event (red). Positives values indicate a northward component and negative values indicate a southward component.

28 have it around 8 m/s and August 24 is the lowest with 2.8 m/s. Upwelling favourable winds were intercalated with some pulses of short southerly winds that happened before the downwelling study case.

Transports across each section are depict in Figure 4.8. An one-directional transport is observed at the shallower external mouths, outflow at north mouth (SP6) and inflow at south mouth (SV2). Main channel sections (SP5, SP3, SP2 and SP1) behave with a two-layered circulation pattern, which during downwelling events have a surface inflow and a deep outflow. Outflow layer extends along all the water column at the north side of the central mouth and in the rest of the section this offshore flow is located from 30 m depth to the bottom. At the middle section (SP3) the transition depth has a great variation and at the inner sections (SP2 and SP1) it is located at 5 m depth.

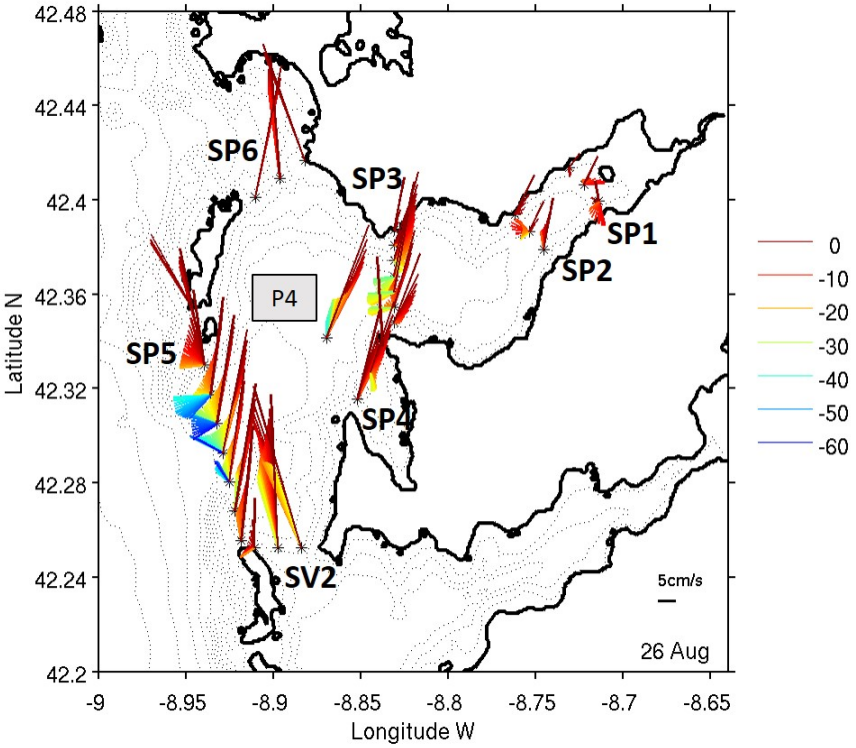

Figure 4.8: Subinertial velocities (cm/s) across sections and station P4 for August 26 at 13 hours. The depth of the arrows correspond to the scale of colors of the colorbar.

The time evolution of the downwelling event can be described using an along-Ría section (Figure 4.9) in a similar way to the upwelling case. Previous days to the downwelling event, upwelling circulation was observed (not described here). At the beginning of the downwelling event, on August 23 (Figure 4.9a,b), anti-estuarine circulation is observed to develop: inshore/offshore flow at surface/deep layers is observed. The river plume seems to be confined to the innermost part of the Ría, as visible in the salinity field (<35.3). This anti-estuarine circulation induces vertical clockwise (CW) circulation cells, centered at -8.89° W and the consequent homogenization of the water column. This occur associated to subduction in a

similar way to the observations of Barton et al. (2016) in Ría de Vigo. One day after the beginning of the downwelling event, August 24, the central Ría is vertically homogeneous, resultant from a vertical mixing. This situation remains the following days, August 25, 26 and 27, with persistent presence of the vertical CW circulation cell centered at -8.86° W on August 25, and displaced to the mouth of the Ría during next days. This cell seems to block the circulation in the middle and inner part, inshore of SP3 section. Last day of the event, August 28, the external blocking lead the river plume to extend until -8.78° W (Figure 4.9k). The consequences of this blocking on the ecosystem will be discussed later.

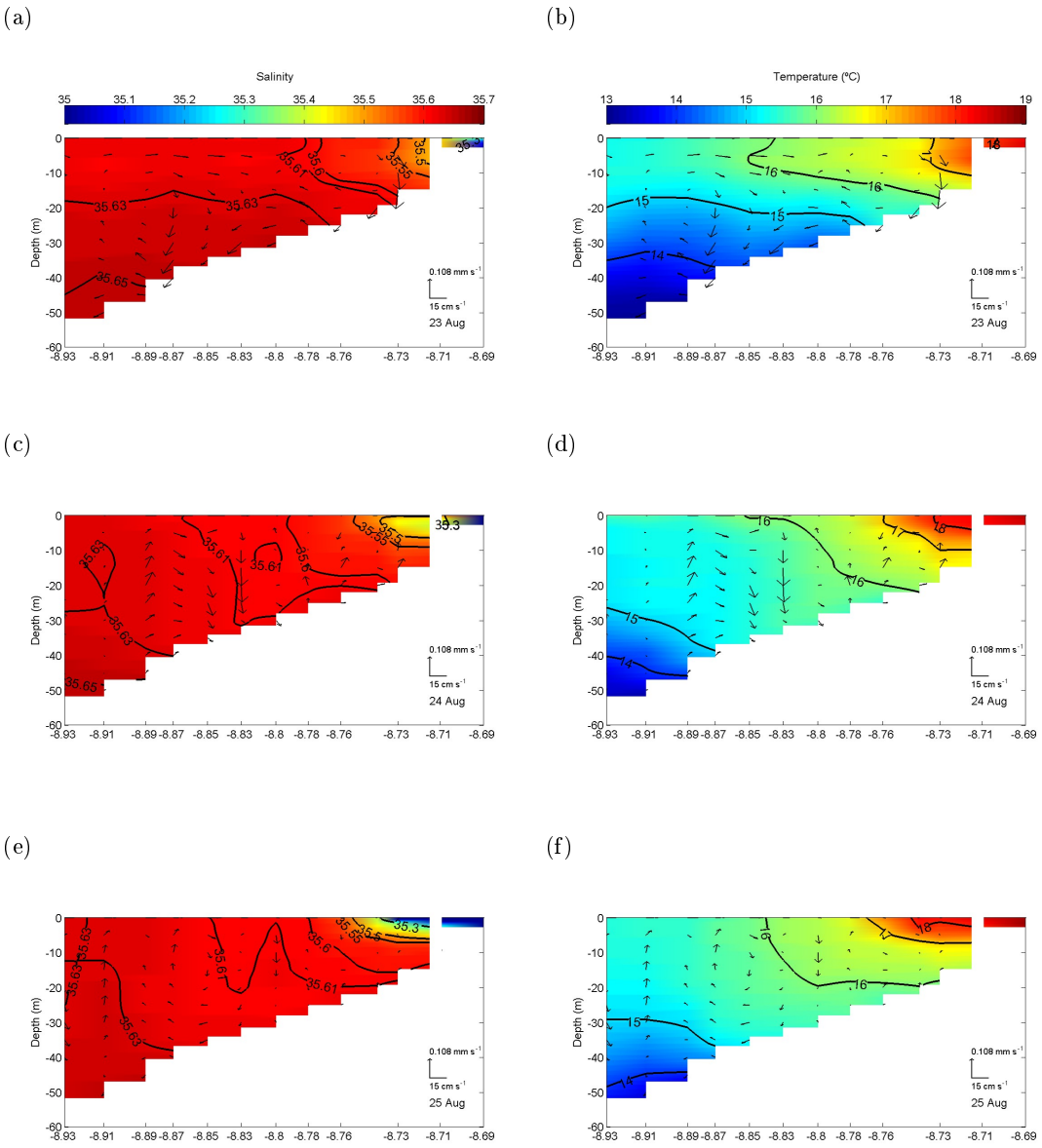

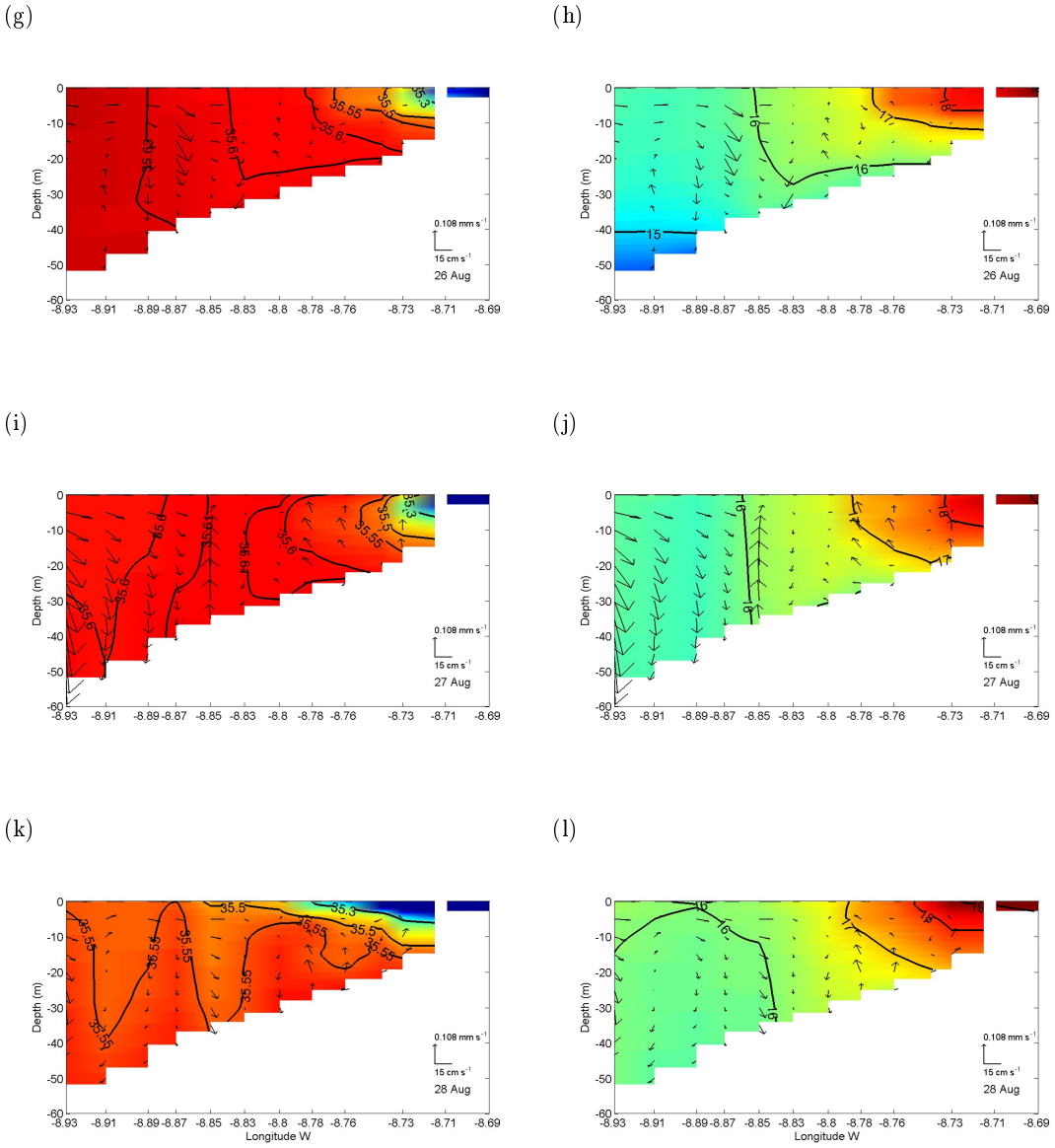

Figure 4.9: Along-Ría section for salinity (a, c, e, g, i, k) and temperature (°C; b, d, f, h, j, l) data with along and vertical subtidal velocities (cm/s and mm/s; black arrows) on August 24, 25, 26, 27 and 28. The sampling transect is shown in Figure 3.3.

4.6 Downwelling Event with River Inflow Increases

A downwelling event was detected in spring during the transition from April to May, exactly from April 29 to May 5, but only five days, from April 30 to May 4, will be studied due to a more clear downwelling circulation. Notice that a Lérez river increase is observed during this period, with a maximum peak on May 4. Prevail directions of wind at this event (Figure 4.10) were southerly and southwesterly, with highest velocities on April 30, May 2 and 4, with 10.6, 13.5 and 14.1 m/s, respectively and lowest velocities on May 1 with 5.3 m/s

and on May 3 with 3.5 m/s. A burst of southerly winds followed by short periods of northerly winds blew some days before the study event.

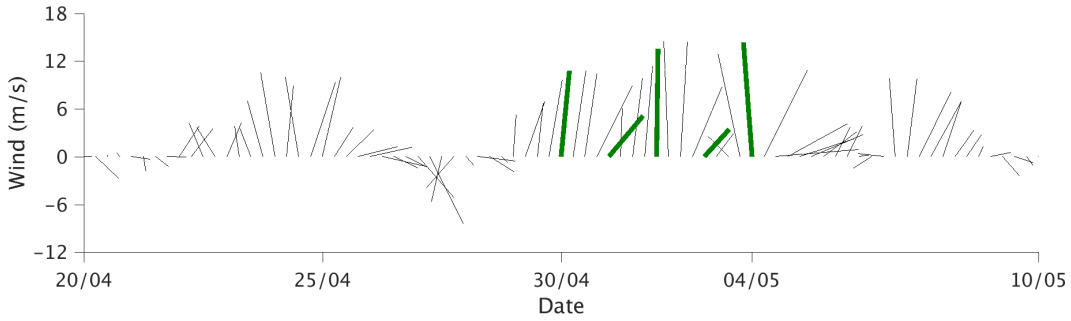

Figure 4.10: Intensities and directions of wind (m/s) during the downwelling event with river flow increase. Positives values indicate a northward component and negative values indicate a southward component.

The flow structure through sections is observed to be similar to those of the previous downwelling event without river flow increase, but some differences are presented at the main channel sections (SP5, SP3, SP2 and SP1; Figure 4.11). At the north zone of the central mouth (SP5), the transition depth is 10 m and at the south zone is 25 m depth. SP3 section has the surface inflow until 10 m depth and below that there is the outflow layer. Inner sections (SP2 and SP1) have the same transition depth as the other events, 5 m depth.

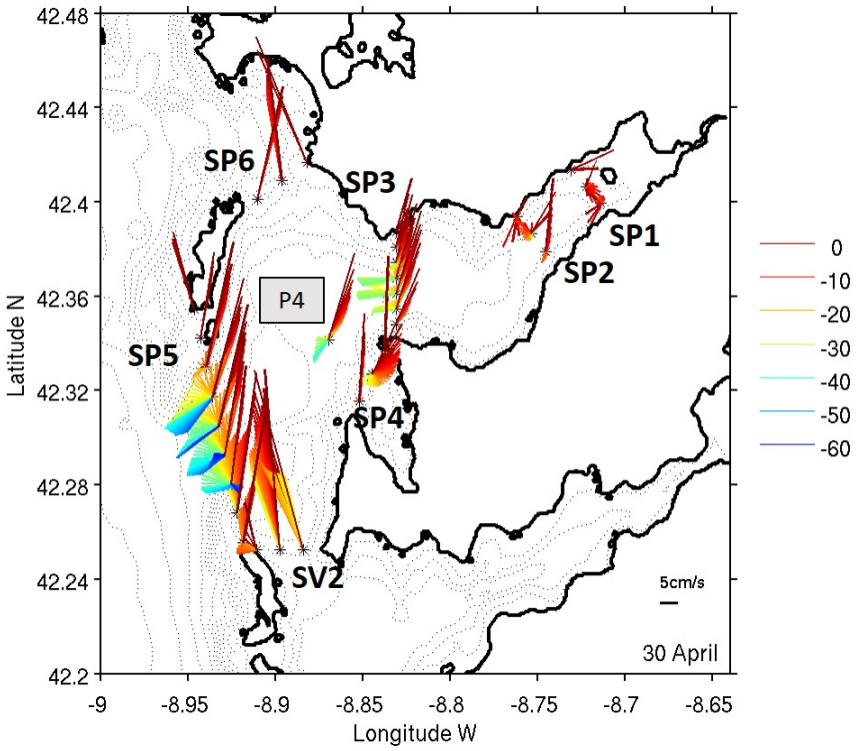

Figure 4.11: Subinertial velocities (cm/s) across sections and station P4 for April 30 at 13 hours. The depth of the arrows correspond to the scale of colors of the colorbar.

To adress the time evolution of the downwelling event with river flow increase (Figure 4.12), an along-Ría section was used to depict T, S and detided velocities (u and w), same as summer upwelling and downwelling events described before. At first day of the study case (Figure 4.12a,b), April 30, the surface inshore flow and the deep offshore flow (anti-estuarine circulation) is shown. At the inner part of the Ría and above 20 m depth vertical mixing is observed and the presence of the river plume is detected near the head of the Ría with salinities values under 31. This vertical mixing extends throughout all the water column and continues the following days, May 1, 2 and 3 with the development of two vertical CW circulation cells. On May 1 these cells are located, one at the mouth (-8.93° W) and other at the middle Ría (-8.84° W). A downwelling of the 15 °C and 35 isolines (Figure 4.12c,d) of about 20 m happens in one day, with an estimated velocity of 0.23 mm/s, which is comparable to the observed velocities. By day May 2, this two cells are displaced inshore, centered at -8.90 and -8.78° W, respectively and the river plume extends until -8.74° W. Stronger vertical mixing is found on May 3, Figure 4.12g,h, and as a consequence a blocking of the circulation is generated, inshore of SP3 section. Last day of this spring downwelling the blocking decreases and the river plume has an offshore movement until -8.75° W.

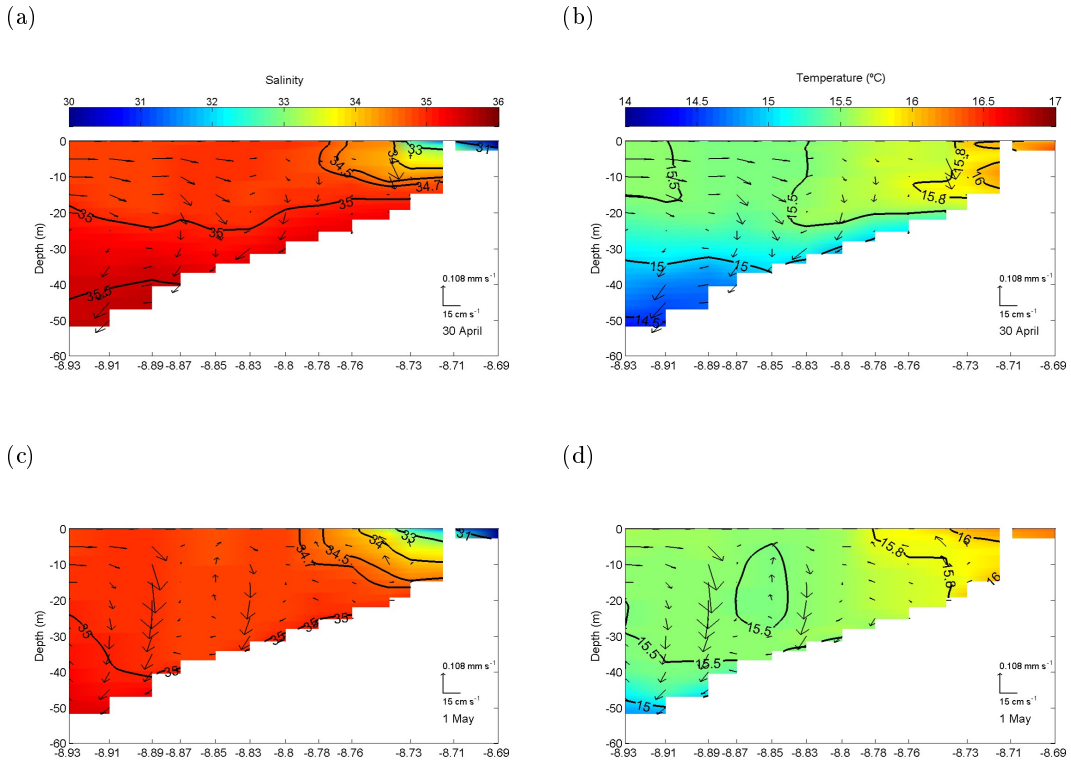

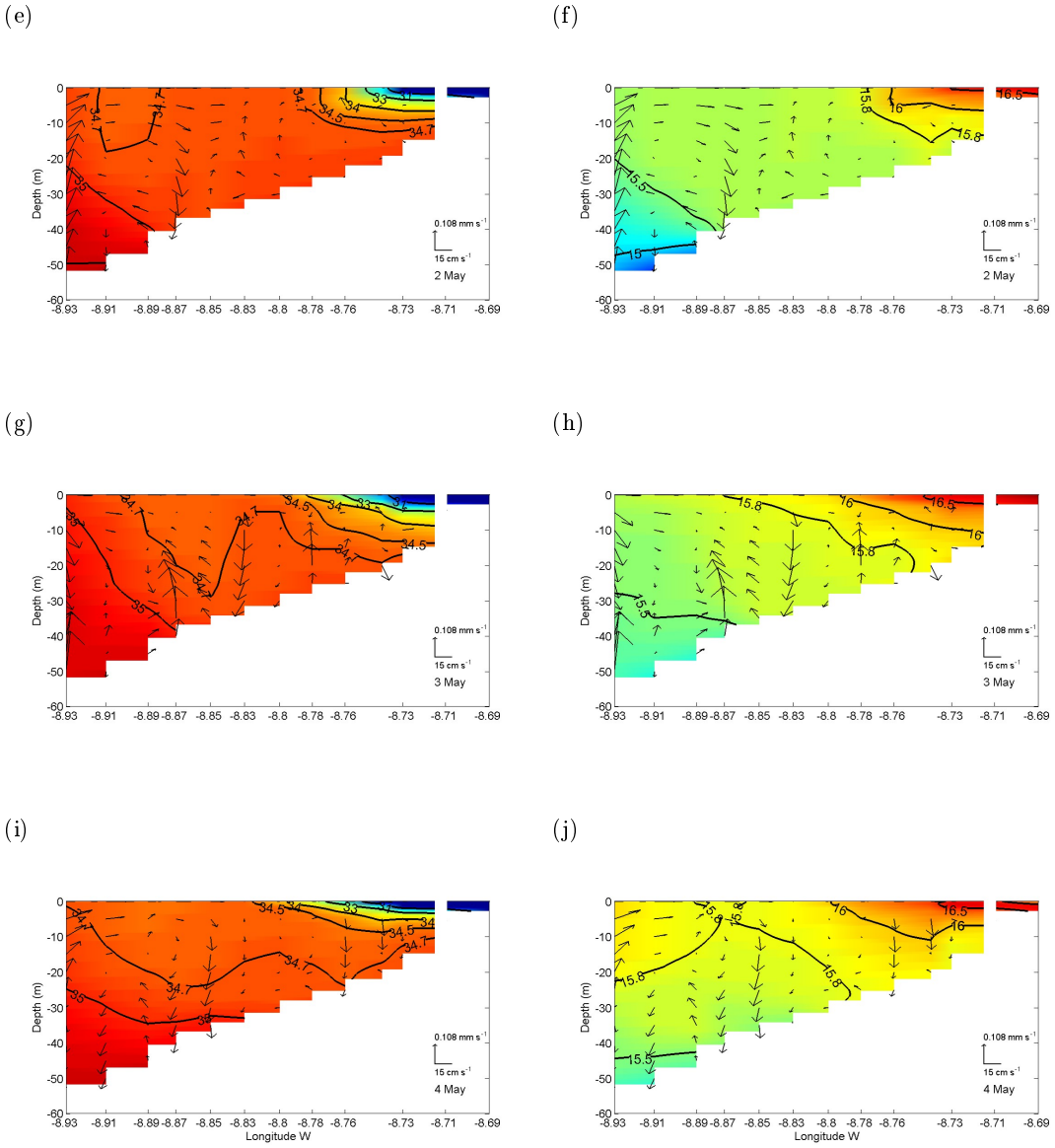

Figure 4.12: Along-Ría section for salinity (a, c, e, g, i) and temperature (°C; b, d, f, h, j) data with along and vertical subtidal velocities (cm/s and mm/s; black arrows) on April 30, May 1, 2, 3, 4. The sampling transect is shown in Figure 3.3.

4.7 Flux and Flushing Time

Fluxes and Flushing times are important physical parameters in estuaries and constitute an useful tool to study the circulation, and exchanges between the estuarine and the coastal ocean. Figure 4.13 shows evolution of yearly flux (In, Out and Total) and flushing time (In and Out) during year 2015 along all the Ría de Pontevedra, through external mouths (Figure 2.2), north (SP6), central (SP5) and south (SV2). Flux (Figure 4.13a) has a high variability,

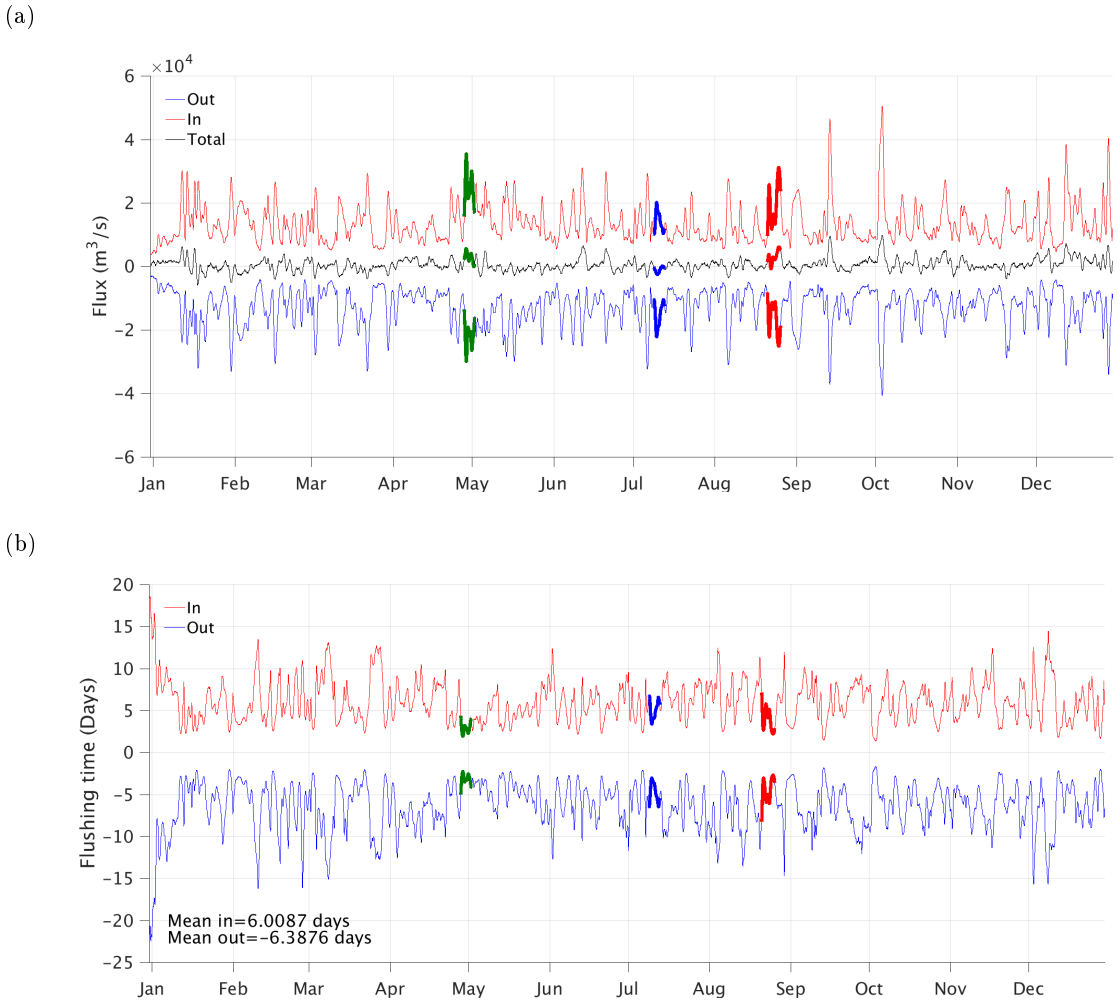

Figure 4.13: Time evolution of (a) Flux and (b) Flushing time for detided data between outermost sections (SP6, SP5 and SV2) and the inner part of the ría (see Figure 2.2). Downwelling event with river flow increase (dark green), upwelling (blue) and downwelling (red) events.

which can depend on the direction and intensity of the wind, location of the oceanic and river waters through the water column, and changes in river flow. In fact, a high correlation, 0.73, between net (total) flux and meridional (V) component of wind exists. Upwelling and downwelling previous study case events (Sections 4.4, 4.5 and 4.6) are represented with colors. Differences of fluxes between upwelling and downwelling events are observed. Net flux has a response for upwelling (negative net flux) and downwelling (positive net flux) events, unlike to the flushing time. Inflow (In) and outflow (Out) fluxes increase during downwelling events, also during these processes changes in direction of wind from southwesterly to southerly generated a decrease in fluxes, as in the spring and summer downwelling events. Existence of two maximum positive peaks of flux are represented in September, 4.5x10^4 m^3/s (inflow), and October, 5x10^4 m^3/s (inflow), with a Lérez river flow around 58 m^3/s for September and about 60 m^3/s for October, and southerly winds with velocities of around 16 m/s (Figure 4.1b) occurred, with associated downwelling events. An increase of 113 m^3/s (Figure 4.2) in

first days of March exists, but it is not a remarkable peak of flux due to an upwelling event that begin on May 3. As we can see the outflow flux tend to be compensated by the inflow flux.

Flushing time, defined in equation 3.18, is depicted in Figure 4.13b and is proportional to the inverse of the flux. It shows upwelling and downwelling modes, but differences between them are not visible. Maximum of flux results in minimum of flushing time, existing a rapid renewal of the water inside the ría. Some examples of that situation occurred in mid-September and first days of October, with flushing times around 2 days. The higher increase in Lérez river flow, 120 m^3/s, gives a flushing time of 4 days, the same as the upwelling event (blue) and higher than for downwelling events, around 1.5 (spring downwelling) and 2 days (summer downwelling). In a general way, a river flow increase is followed by an increase in the flux and a decrease in the flushing time because the Ría needs a short period to flush it.

Linear correlations between inflow and outflow flushing times versus both components of wind and rivers flow are depict in Figure 4.14. Almost along all the year exists a good correlation with meridional (V) component of wind, being higher for outflow flushing time and having a continuous correlation, of around 0.5, during summer months, July and August. Average of rivers flow have a high correlation with flushing times, this good correlation occur when southerly winds prevailed and there is an increase in rivers flow, obtaining short flushing times, as from September to mid-October and in December.

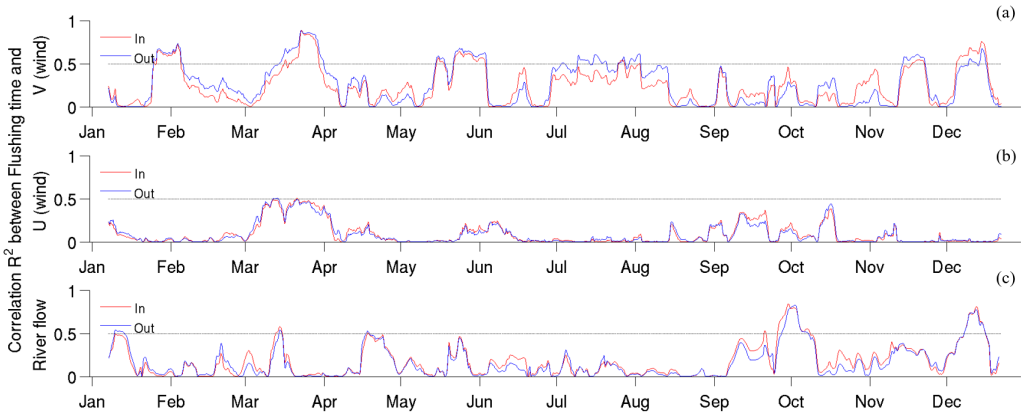

Figure 4.14: Time evolution of the linear correlations R^2 for a moving window of 15 days for detided data between Flushing time and (a) the meridional (V) component of wind, (b) the zonal (U) component of wind and (c) the average of the rivers flow (Lérez, Verdugo and Miño rivers)

4.8 Empirical Orthogonal Functions (EOFs)

EOFs analysis are a valuable statistical tool, that allow not only to evaluate circulation pattern at Ría de Pontevedra, but also gives a general portrait of that variability. In this study it was applied to detided normal velocity data for each section (SP6, SP5, SV2, SP3, SP2 and SP1; Figure 2.2). From preliminary results, it is quite obvious that the main mode of variability for subinertial normal velocities is produced by winds. However, other forcings

could also be important, as increase in rivers flow (Lérez, Verdugo and Miño). Out of 60 possible EOFs modes, the first three modes contributed 77% variance for detided normal velocities. The first mode accounted for 60.4% of the variance, the second mode 12.64% and the third 3.98%. For simplicity, we only describe the first two modes, depicted in Figures 4.15 and 4.16. The time series of Figures 4.15 and 4.16 are normalized, i.e. the mean value was subtracted, and the result was divided by the standard deviation, in such a way that the correlation of this series with other variables (also normalized) can be easily viewed.

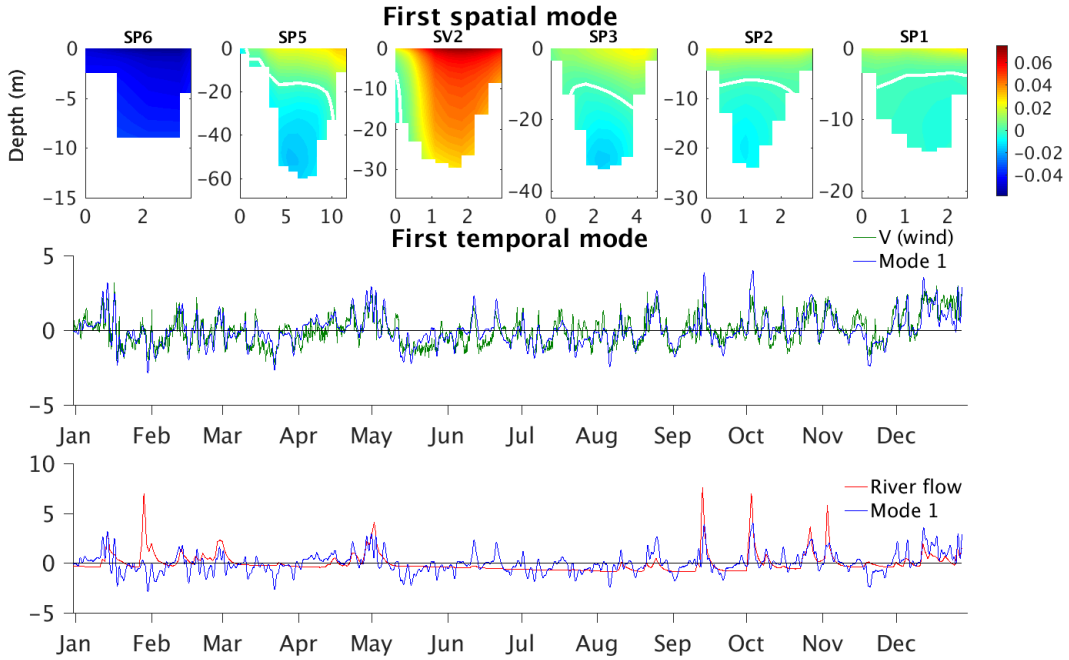

Figure 4.15: EOF first spatial (upper graphic) and normalized temporal modes for the normal detided velocity versus meridional (V) component of wind (center graphic) and average of river flows (Lérez, Verdugo and Miño rivers; lower graphic).

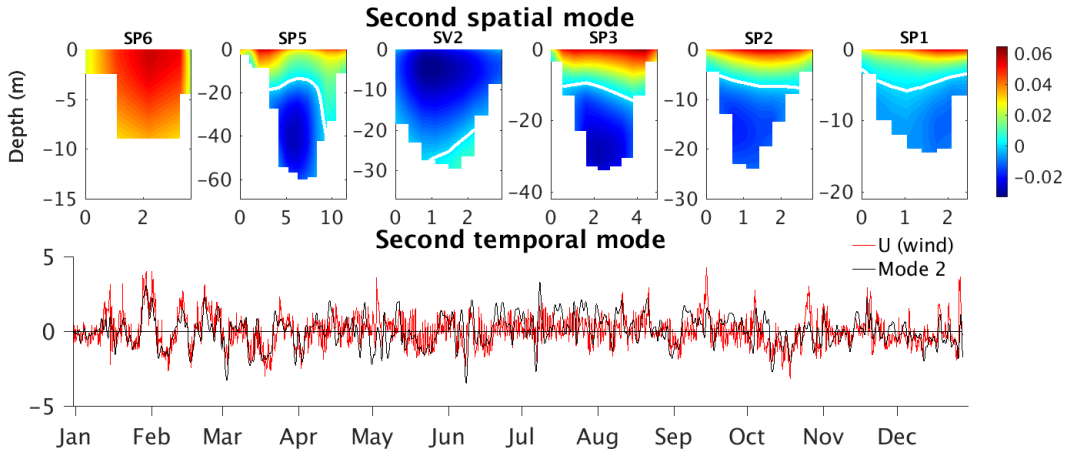

Figure 4.16: EOF second spatial (upper graphic) and normalized temporal modes for the normal detided velocity versus zonal (U) component of wind (lower graphic).

The first and second modes of variability (Figures 4.15 and 4.16) represents basically a downwelling/upwelling circulation characterized by an outflow/inflow at north mouth (SP6), an inflow/outflow at south mouth (SV2). At along Ría sections (SP5, SP3, SP2 and SP1; Figure 2.2), the pattern is dominated by a two-layer circulation with a level of no motion separating surface inflow/outflow and deep outflow/inflow. The level of no motion varies its location throughout the section and at different sections, depending on its depth. North mouth do not have this level due to its shallowness, south mouth has it only in its west side, with a vertical orientation and in rest of sections it varies from 5 m to 10 m depth for middle (SP3) and innermost (SP2 and SP1) sections and from 10 to 30 m depth for central mouth (SP5).

First EOF temporal serie (Figure 4.15) correlates with the meridional (V) wind component and the second EOF temporal serie correlates with the zonal (U) component of wind. Positives values of meridional component and first temporal mode correspond with southerly winds and result in downwelling events with outflow and inflow through north and south mouth, respectively and superficial inflow and bottom outflow at along Ría sections. The opposite case is observed under northerly winds, when negative values of mode 1 and V component of wind are represented and as a consequence upwelling events are identified by inflow and outflow through north and south mouth, respectively and surface outflow and deep inflow at SP5, SP3, SP2 and SP1 sections. Second temporal mode (Figure 4.16) represents the zonal (U) component of wind, positive values indicate westerly winds and negative indicate easterly winds. Westerly winds (positive values of mode 2) produce an inflow of the waters at the surface and a deep outflow at the sections located in the main channel of the Ría. North and south mouth have an inflow and an outflow, respectively. Easterly winds or negative values of mode 2 force waters to leave the estuary through surface layers and to enter at the deep layers for along Ría sections, whilst north and south mouth have a behaviour that is characteristic of downwelling events, outflow at SP6 and inflow at SV2. First EOF temporal serie, also explains reasonably the increase on the average rivers flow, as in mid September and beginning of October. It can result as a consequence of southerly winds (first temporal mode) that exert a transport of estuarine waters from Ría de Vigo to Ría de Pontevedra during downwelling favourable winds.

Table 4.2: Linear correlation coefficients between time series of mode 1, 2 and 3 versus upwelling index, meridional (V) and zonal (U) components of wind and rivers flow for Lérez, Verdugo and Miño.

	Upwelling Index	**V (wind)**	**U (wind)**	**Rivers**		
				Lérez	**Verdugo**	**Minho**
Mode 1	-0.81	0.82	0.11	0.23	0.49	0.18
Mode 2	-0.11	0.2	0.57	-0.16	-0.04	0.03
Mode 3	-0.08	0.14	-0.06	0.21	0.01	0.16

Table 4.2 shows linear correlations between three first temporal modes versus upwelling index (UI), defined in equation 3.21, for both component of wind (U and V) and rivers flow

(Lérez, Verdugo and Miño). Positive values of the UI correspond with upwelling events and negative values with downwelling events. Mode 1 have a correlation of 0.82 with V component of wind and 0.49 with Verdugo river. Mode 2 has a significant linear correlation of 0.57 with U component of wind. No others significant correlations were achieved for all others modes and variables. Linear correlations R^2 for these modes with components of winds and rivers flow were computed in Figure 4.17.

Linear correlations R^2 between the first and second time EOF series versus both component of wind and the average of rivers flow (Lérez, Verdugo and Miño) are shown in Figure 4.17. The mode 1 is well correlated with meridional component of wind during all the study period and with the average of rivers flow from middle September until middle October. In this period, peaks of Verdugo flow and maximum values of the first temporal mode occur. A high dependency exists between the meridional component of wind and the transport of water from Ría de Vigo to Ría de Pontevedra. The mode 2 has a significant correlation during first three months with zonal component of wind and around 0.5 in January and February with the average of rivers flow, which is related with high values of the flows and mode 2 during this period. In June/July, the correlations are near 0.5 with both components of wind and at the end of the year, only, with U component. Also, a good correlation between mode 2 and the zonal component of winds is shown.

(a)

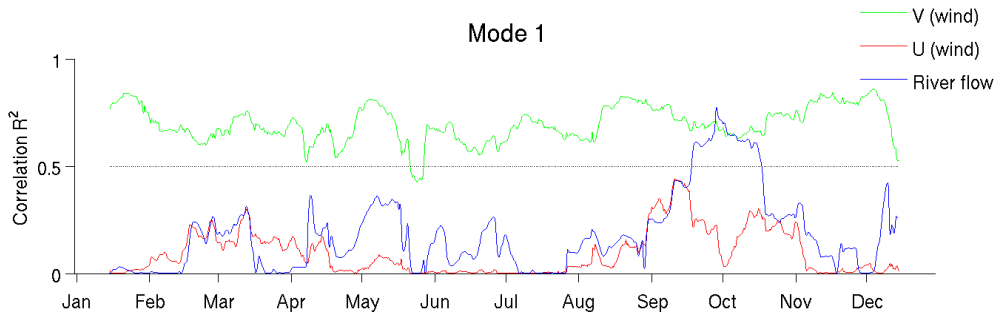

(b)

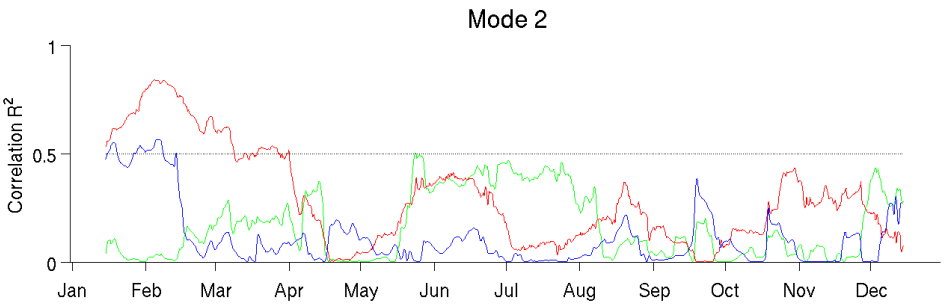

Figure 4.17: Time evolution of the linear correlations R^2 for a moving window of 30 days between the (a) first and (b) second modes and the meridional (V) component of wind, the zonal (U) component of wind, and the average of the rivers flow (Lérez, Verdugo and Miño rivers).

5. Discussion

The circulation pattern in the Ría de Pontevedra is characterized by the alternancy of positive estuarine circulation, enhaced during upwelling events and negative estuarine circulation or downwelling events. It is affected by the wind directions and the river inflow increases. In this thesis a summer upwelling event and two downwelling events, one in summer and the other in spring with a river inflow increase were analyzed. The exchange of waters and their circulation inside the Ría, is an important factor to control and enhance the production in the aquaculture of the zone, as mussels production. The results of a three-dimensional model (ROMS-AGRIF) configurated in the framewrok of Mytiga project were used.

The upwelling events (Figure 5.1a) respond with an inflow throughout the north mouth (SP6), outflow throughout the south mouth (SV2) and a surface outflow and a deep inflow at the main channel (SP5, SP3, SP2 and SP1). In contrast, the downwelling events (Figure 5.1b) are characterized by an outflow/inflow through the north/south mouths and a surface inflow and a deep outflow along the main channel. The central mouth (SP5) responds with a surface inshore flow at the central and south sides, and an offshore flow at the deep layers, increased at the northern side of the mouth, near Ons island. This pattern coincides with the one observed by Aguiar Fernandez (2016) at the Ría de Pontevedra through the north, central and south mouths, with exception of the northern side of the central mouth, which was not displayed in her study.

Lérez river plume typically extend until the middle part of the Ría de Pontevedra during upwelling events. During strong southerly winds or downwelling events the waters from Ría de Vigo can enter into Ría de Pontevedra through the south mouth (SV2). Also, during these events the Lérez river waters can extend to the middle part of the Ría due to a blocking, located between SP5 and SP3, likely associated to the vertical clockwise circulation cell. Examples of this vertical cell can be seen in both downwelling examples, and the presence of this front is described by Pardo et al. (2001) for the Ría de Pontevedra, and by Barton et al. (2016) and Villacieros-Robineau et al. (2013) for Ría de Vigo.

A surface stratification of the waters occurs from July 12 to 15 (upwelling event), and at the deeper layers the uplift of the isohalines and the isotherms is visible, with a deep inshore flow during the event (Barton et al., 2015) in response to the offshore surface Ekman transport. When southerly winds blew, a subduction of the estuarine waters is observed (Barton et al., 2015, 2016), and led to a nearly uniform vertical structure of thermohaline properties, which is reinforced under river inflow increase, from May 1 to 4, as described above (Section 4.6).

As seen by other authors Barton et al. (2015, 2016); de Castro et al. (2000), this blocking of the waters can be the origin of the "red tides", consequence of the export of nutrients from the benthic environment to all the water column through a vertical mixing, which contribute to the primary production within the Ría.

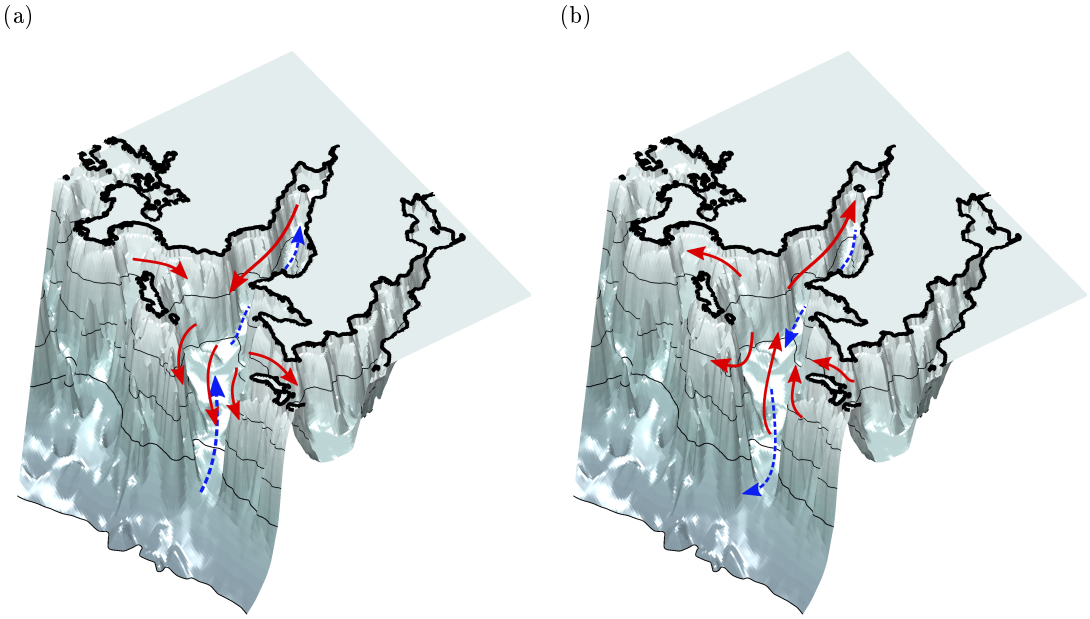

Figure 5.1: Circulation pattern at Ría de Pontevedra for (a) upwelling events and (b) downwelling events. Red arrows represent surface flows and blue dashed arrows represent deep flows. Isobaths are shown at 20 m, 40 m, 60 m and 100 m depth.

In order to characterize the exchange of waters between the Ría and the adjacent shelf and the time scale of renewal, the fluxes and the flushing times were studied for year 2015. Maximum peaks of fluxes are found during downwelling events rather than upwelling events. When these downwelling events occur at the same time as river inflow increase, higher fluxes are observed. By contrast, flushing time do not present recognizable differences between upwelling and downwelling events, but shorter times are observerd at the two downwelling events studied than at the upwelling events. This higher flushing times during the upwelling event, can be a consequence of the decrease of the deep inflow velocities due to the friction.

A statistical tool was computed, EOFs analysis, to study the variability of the inshore and offshore flows and their correlations with different variables. Under northerly (negative mode 1)/southerly (positive mode 1) wind directions, an inflow/outflow is observed at the north mouth (SP6), an outflow/inflow is observed at the south mouth (SV2) and the main channel sections respond with a surface outflow/inflow and a deep inflow/outflow. Mode 2 represents westerly (positive mode 2)/easterly (negative mode 2) wind directions. Westerly winds produced an inflow at the north mouth, an outflow at the south mouth and at the principal longitudinal axis of the Ría, the estuarine waters enter the Ría through the surface and are force to leave the Ría at the deep layers, opposite respond occurs under easterly

winds. Similar behaviour was observed by de Castro et al. (2000) under westerly and easterly winds and by Aguiar Fernandez (2016) for both modes.

As we can see, similar circulation patterns obtained in this thesis were described by others authors for other periods, so we can conclude that the model has a good representation of the processes occurring inside the Ría. A coupling of this model with a biogeochemical one can be done to achieve a better comprehension of the processes that leads to HABs generation and the general trend of the circulation patterns at Ría de Pontevedra can will be studied with an increase in the analyzed years.

6. Conclusions

Although it has long been recognized that the rías respond with two typical circulations, upwelling or positive estuarine circulation and downwelling or negative estuarine circulation, the detail of the present results provide new insights about the general estuarine circulation at Ría de Pontevedra.

The surface layer outflow and the deep layer inflow occur during the upwelling events at the main channel, whilst the north and south mouths fluxes are controlled by the coastal jet associated to the wind forcing, observing an inflow/outflow through the northern/southern mouths. When the upwelling is well established, the stratification of the surface increased and the offshore advection of the river plume is observed until the middle Ría. If upwelling favourable winds follow a downwelling event with river inflow increase, the river waters can spread along the Ría through the northern and central mouths, while the southern mouth is characterized by the inflow of waters from Ría de Vigo.

The downwelling events are characterized by a surface inflow and a deep outflow at the main channel and at the northern and southern mouths there is an outflow and inflow, respectively. Onshore flow of surface waters associated to southerly winds generate a vertical mixing of the water column, and a vertical clockwise circulation located between the outer and middle parts of the Ría, which create a region that seems to isolate the waters at the inner part of the Ría, and create the environment responsible for the production of HABs. These negative estuarine circulation have maximum peaks of flux, which increase when a river inflow increase occur. Flushing times are short, around 2 days.

The statistical tool used to support this study was the EOFs, applied to the subinertial velocity fields across sections of the Ría. The first and second modes of variability represent the winds forced for the upwelling and downwelling circulations. Northerly (negative mode of temporal serie) and southerly winds (positive mode of temporal serie) are represented by the mode 1, and describe the characteristic circulation for downwelling and upwelling events, respectively. Westerly (positive mode of temporal serie) and easterly (negative mode of temporal serie) wind directions are represented by the mode 2. Westerly directions of wind described a surface inflow and as a consequence a deep outflow occur. On the contrary, easterly winds force waters to leave the estuary through the surface layers and to enter it through the deep layers.

The Ría de Pontevedra as other Rías, has a great importance for the mussel production industry. If forecast of HABs events are to be achieved, a coupling of physical and biogeo-

chemical models is neccesary to understand the principal causes that generate these events in order to prevent it and to counteract it in some way. This work contributes to the forecast of the physical conditions associated to the set-up of HABs.

Bibliography

Aguiar Fernandez, Eva (2016), Circulation at the transition zone between the shelf and the two southernmost Rías Baixas (NW Spain), PhD thesis, University of Vigo.

Álvarez, I, M DeCastro, R Prego and M Gómez-Gesteira (2003), 'Hydrographic characterization of a winter-upwelling event in the Ria of Pontevedra (NW Spain)', *Estuarine, Coastal and Shelf Science* **56**(3-4), 869–876.

Alvarez, I, M Gomez-Gesteira, M Decastro and E M Novoa (2008), 'Ekman transport along the Galician Coast (NW, Spain) calculated from QuikSCAT winds', *Journal of Marine Systems* **72**, 101–115.

Barton, E. D., J. L. Largier, R. Torres, M. Sheridan, A. Trasviña, A. Souza, Y. Pazos and A. Valle-Levinson (2015), 'Coastal upwelling and downwelling forcing of circulation in a semi-enclosed bay: Ria de Vigo', *Progress in Oceanography* **134**, 173–189.

Barton, E. D., R. Torres, F. G. Figueiras, M. Gilcoto and J. Largier (2016), 'Surface water subduction during a downwelling event in a semienclosed bay', *J. Geophys. Res. Oceans* **121**, 1063–1084.

Bender, Vera B., Till J. J. Hanebuth, Anxo Mena, Karl-Heinz Baumann, Guillermo Francés and Tilo von Dobeneck (2012), 'Control of sediment supply, palaeoceanography and morphology on late Quaternary sediment dynamics at the Galician continental slope', *Geo-Marine Letters* **32**(4), 313–335.

Berx, B., M. Dickey-Collas, M.D. Skogen, Y.-H. De Roeck, H. Klein, R. Barciela, R.M. Forster, E. Dombrowsky, M. Huret, M. Payne, Y. Sagarminaga and C. Schrum (2011), 'Does operational oceanography address the needs of fisheries and applied environmental scientists?', *Oceanography* **24**(3), 166–171.

Daily, Gretchen C., Susan Alexander, Paul R. Ehrlich, Larry Goulder, Jane Lubchenco, Pamela A. Matson, Harold A. Mooney, Sandra Postel, Stephen H. Schneider, David Tilman and George M. Woodwell (1997), 'Ecosystem Services: Benefits Supplied to Human Societies by Natural Ecosystems', *Issues in Ecology* **2**, 1–12.

Dale, A W, R Prego, G E Millward and M Gomez-Gesteira (2004), 'Transient oceanic and tidal contributions to water exchange and residence times in a coastal upwelling system in the NE Atlantic: the Pontevedra Ria, Galicia', *Marine Pollution Bulletin* **49**, 235–248.

de Castro, M., M. Gómez-Gesteira, I. Alvarez and R. Prego (2004), 'Negative estuarine circulation in the Ria of Pontevedra (NW Spain)', *Estuarine, Coastal and Shelf Science* **60**(2), 301–312.

de Castro, M, M Gómez-Gesteira, R Prego, J J Taboada, P Montero, P Herbello and V Pérez-Villar (2000), 'Wind and Tidal Influence on Water Circulation in a Galician Ria (NW Spain)', *Estuarine, Coastal and Shelf Science* **51**, 161–176.

Debreu, Laurent, Patrick Marchesiello, Pierrick Penven and Gildas Cambon (2012), 'Two-way nesting in split-explicit ocean models: Algorithms, implementation and validation', *Ocean Modelling* **49-50**, 1–21.

Díaz, Patricio A, Manuel Ruiz-Villarreal, Lourdes Velo-Suárez, Isabel Ramilo, Patrick Gentien, Michel Lunven, Liam Fernand, Robin Raine, Beatriz Reguera and Patricio A Diaz (2014), 'Tidal and wind-event variability and the distribution of two groups of Pseudo-nitzschia species in an upwelling-influenced ría', *Deep-Sea Research Part II: Topical Studies in Oceanography* **101**, 163–179.

Egbert, Gary D and Svetlana Y Erofeeva (2002), 'Efficient inverse modeling of barotropic ocean tides', *J. Atmos. Ocean. Tech.* **19**, 183–204.

Evans, Graham and Ricardo Prego (2003), 'Rias, estuaries and incised valleys: is a ria an estuary?', *Marine Geology* **196**(3-4), 171–175.

Gómez-Gesteira, M, M de Castro, R Prego and V Pérez-Villar (2001), 'An unusual two layered tidal circulation induced by stratification and wind in the Ria of Pontevedra (NW Spain)', *Estuarine, Coastal and Shelf Science* **52**(5), 555–563.

Gómez-Gesteira, M., M. DeCastro and R. Prego (2003), 'Dependence of the water residence time in Ria of Pontevedra (NW Spain) on the seawater inflow and the river discharge', *Estuarine, Coastal and Shelf Science* **58**(3), 567–573.

Gomez-Gesteira, Moncho, Camilo Moreira, Ines Alvarez and Maite DeCastro (2006), 'Ekman transport along the Galician coast (northwest Spain) calculated from forecasted winds', *Journal of Geophysical Research* **111**(C10), C10005.

González-Quijano, A., J.M. Cabanas, J.J. González and F. Schultze (1991), 'Datos químico–oceanográficos de la Ría de Pontevedra en invierno. Parte II', *Infor. Téc. Inst. Esp. Oceanogr.* .

Mann, K. H. and J. R Lazier (2006), *Dynamics of marine ecosystems. Biological–Physical Interactions in the Oceans*, 3rd editio edn, Blackwell Publishing Ltd. ISBN: 9781405111188.

Marta-Almeida, Martinho and Jesús Dubert (2006), 'The structure of tides in the Western Iberian region', *Continental Shelf Research* **26**(3), 385–400.

Nolasco, R., S.E. Swearer, I. Gomes, L. Peteiro, R. Albuquerque, T. Luna, J. Dubert and H. Queiroga (in review), 'The known unknowns: accounting for uncertainty improves cross-validation of independent estimates of marine population connectivity', *Scientific Reports* p. 5.

Nolasco, Rita, Ana Cordeiro Pires, Nuno Cordeiro, Bernard Le Cann and Jesus Dubert (2013), 'A high-resolution modeling study of the Western Iberian Margin mean and seasonal upper ocean circulation', *Ocean Dynamics* **63**(9-10), 1041–1062.

Oceana (2009), Propuesta de áreas marinas de importancia ecológica (zona galaico-cantábrica), Technical report.

Pardo, P C, M Gilcoto and F F Pérez (2001), 'Short-time scale coupling between termohaline and meteorological forcing in the Ría de Pontevedra', *Scientia Marina* **65**(1), 229–240.

Penven Pierrick (2000), A numerical study of the Southern Benguela circulation with an application to fish recruitment., PhD thesis, University of Bretagne Occidentale.

Pielke, Roger A. (2013), *Mesoscale meteorological modeling*, 3rd edn, Elsevier. ISBN: 0125547668.

Prego, R, A W Dale, M de Castro, M Gómez-Gesteira, J J Taboada, P Montero, M R Villareal and V Pérez-Villar (2001), 'Hydrography of the Pontevedra Ria: Intra-annual spatial and temporal variability in a Galician coastal system (NW Spain)', *Journal of Geophysical Research C: Oceans* **106**(C9), 19,845–19,857.

Preisendorfer, R.W. and C.D. Mobley (1988), *Principal component analysis in meteorology and oceanography*. ISBN: 0444430148.

PROVIGO (1996), Nueve Años de Muestreo Hidrográfico en la Ría de Vigo (Enero 1987-Enero 1996), Technical report.

Rios, Aida F., Fiz F. Pérez and F. Fraga (1992), 'Water masses in the upper and middle North Atlantic Ocean east of the Azores', *Deep Sea Research Part A, Oceanographic Research Papers* **39**(3-4), 645–658.

Ruiz-Villarreal, M, P Montero, J J Taboada, R Prego, P C Leitao and V Perez-Villar (2002), 'Hydrodynamic Model Study of the Ria de Pontevedra Under Estuarine Conditions.', *Estuarine, Coastal and Shelf Science* **54**, 101–113.

Shchepetkin, Alexander F and James C McWilliams (2003), 'A method for computing horizontal pressure-gradient force in an oceanic model with a nonaligned vertical coordinate', *Journal of Geophysical Research* **108**(C3), 1–42.

Shchepetkin, Alexander F. and James C. McWilliams (2005), 'The regional oceanic modeling system (ROMS): A split-explicit, free-surface, topography-following-coordinate oceanic model', *Ocean Modelling* **9**(4), 347–404.

Villacieros-Robineau, N, J L Herrera, C G Castro, S Piedracoba and G Roson (2013), 'Hydrodynamic characterization of the bottom boundary layer in a coastal upwelling system (Ría de Vigo, NW Spain)', *Continental Shelf Research* **68**(October 2013), 67–79.

Willmott, C. J. (1981), 'On the validation of models', *Physical Geography* **2**(2), 184–194.